von KARMAN INSTITUTE

FOR FLUID DYNAMICS

Technical Note 177

CYCLE COUNTING FUNCTION OF TSI 1990A AND 1980 LDV PROCESSORS AS A MEANS OF PARTICLE TRANSIT TIME MEASUREMENT

F. Leprince

June 1991

RHODE SAINT GENESE BELGIUM

D/1991/0238/393

VKI TN 177

von Karman Institute for Fluid Dynamics
Chaussée de Waterloo, 72
B–1640 Rhode Saint Genèse–Belgium

Technical Note 177

CYCLE COUNTING FUNCTION OF TSI 1990A AND 1980 LDV PROCESSORS AS A MEANS OF PARTICLE TRANSIT TIME MEASUREMENT

F. Leprince

June 1991

Table of Contents

ABSTRACT

The cycle-counting function of LDV processors provides a means of measuring the transit time of a seed particle in the probe volume in order to correct velocity bias and velocity gradient errors by weighting individual velocity measurements by the transit time. The main objectives of the investigation are to study the dependence of the number of counted cycles on signal level, and to check that the cycle-counting process is independent of the doppler frequency. Tests of TSI 1990A and 1980 counters are performed with different kinds of simulated signals generated by function generators. Measurements show that the number of counted cycles depends on the ratio of signal to threshold detector levels in a predictable way. The cycle-counting process is not frequency dependent, so that no bias will be introduced on weighted velocity measurements; indirect accuracy limitations will unavoidably arise from the dispersion introduced by the effect of signal level. Major difficulties have been encountered because the signals used for test purposes were different from actual LDV signals, causing wrong cycle-counts: occurrence of end-of-burst failure due to improper signal shape, and interference of the dead time of the processor with cycle-counting. Other difficulties are related with signal shape imperfections. In actual measurements errors of the same kind are likely to occur owing to the lack of validation of cycle-counts. Requirements for a suitable cycle-counting processor, as well as the conditions of proper signal generation for testing doppler processors are defined.

LIST OF SYMBOLS

N	Number of cycles delivered at the output of the processor
N_m	Number of cycles preset by the operator
N_t	Number of cycles timed to measure the doppler period
N_{tr}	Number of cycles above threshold
T	Time delivered at the output of the processor
T_D	Doppler period
T_m	Time envelope corresponding to N_m preset cycles
T_{tr}	Time envelope corresponding to signal above threshold

Abbreviations

AM	Amplitude Modulation
BPR	Burst Presence Ratio
CEI	Commodore Extension Interface
DAS	Data Acquisition System
DSS	Doppler Signal Simulator
EOB	End-Of-Burst
ERM	Ecole Royale Militaire
FFT	Fast Fourier Transform
HF	High Frequency
IC	Input Conditioner
LDV	Laser Doppler Velocimetry
LF	Low Frequency
MR	Modulation Ratio
NC	N-Cycle
PIA	Peripheral Interface Adapter
pp	peak-to-peak
SMB	Single Measurement per Burst
SNR	Signal to Noise Ratio
TB	Total Burst

1. INTRODUCTION

1.1 Transit time weighting

Velocity measurements by LDV are believed to exhibit systematic errors [1] in highly fluctuating flows or in large velocity gradients, because the seed particle rate may be assumed proportional to the local, instantaneous velocity of the flow.

In fluctuating flows, the particle rate is higher when the velocity is high; more high velocity particles are measured; the probability density of particle velocity is, compared to that of flow velocity, biased towards higher velocities. This is the velocity bias problem.

In the same way, more particles are likely to be measured in the high velocity region of the measuring volume in a velocity gradient. Even in a symmetrical volume, the particle averaged velocity is higher than the velocity at the center of the volume. This is the velocity gradient error.

George [2,3] proved on theoretical grounds, that the troublesome effect of proportionality between the particle rate and the velocity could be corrected by weighting every individual velocity measurement by the transit time, i.e., the residence time of the particle in the measuring volume, provided only one measurement is allowed per seed particle. In a velocity gradient, a spatially averaged measurement is obtained, which reduces to the velocity at the center of a symmetrical volume as long as it is not truncated, e.g. by the wall in a boundary layer.

The weighted velocity $< U >$ and fluctuation $< u^2 >$ are obtained from individual velocity and transit time measurements U_i, T_i by :

$$< U >= \frac{\sum U_i T_i}{\sum T_i}$$

$$< u^2 >= \frac{\sum (U_i - < U >)^2 T_i}{\sum T_i}$$

1.2 Measuring the transit time

The transit time of a particle can be obtained by measuring the length of the doppler burst generated by this particle. On counter type processors the transit time is obtained as the product of the number of doppler cycles and of the doppler period. In addition to the determination of the period, the processor must be provided with a cycle-counting function.

1.3 Statistical independence of the number of counted cycles

In a quite general way, correct weighted averages can only be obtained if the cycle-counting process is actually independent of the velocity of the particle. In this case, the number of counted cycles is statistically independent of the velocity of the particle, and transit time weighted quantities are not biased. In particular, attention must be paid to the way the cycle-counting process depends on the level of the signal on the TSI processor.

1.4 Cycle-counting function and signal level

Transverse light intensity profiles in ideal laser beams have gaussian shapes. Consequently, there is neither an absolute number of fringes in a measuring volume nor an absolute number of cycles in a doppler signal. Usually, the number of cycles is defined between e^{-2} levels of the peak value. To obtain representative doppler burst lengths, it is sufficient to count at a fixed relative level which may be different from the e^{-2} level.

As in the TSI counter the counting process is initiated by a fixed threshold on signals pre-processed with a constant gain, this condition is not satisfied. Considering two signals containing the same number of cycles, the strong signal is detected near the bottom, many cycles are counted (Fig. 1a); the weak signal near the top, few cycles are counted (Fig. 1b).

The origin of the differences in signal level is either the size of the scattering particle, or the path it follows in the measuring volume. It has been proven [2,3] that the influence of the latter has no effect on transit time weighted averages.

As long as the signal level may be considered as independent of the velocity of the particle, the dispersion it introduces in the measured transit time does not bias the weighted quantities. The fact that the number of counted cycles depends on the level of the signal induces, however, indirect limitations of the accuracy of the process of transit time weighting :

- A larger number of individual measurements is needed to average out the transit time dispersion induced by the effect of signal level on the number of measured cycles [4];
- The small numbers counted on weak signals are inherently less accurate than large numbers on strong signals; this difficulty can be overcome by frequency shifting.

1.5 Objectives

Measurements are carried out to study the cycle-counting function of the TSI counter. Tests are performed using synthetic doppler signals produced by function generators. The parameters of the study are the level of the signal, the doppler frequency and the number of cycles in a burst. The effect of signal level on cycle-counting is measured and compared

to the behaviour described in the preceding section. Whether the cycle-counting process depends on the velocity or not is checked by varying the doppler frequency at constant signal level. In addition the accuracy of frequency measurements is measured.

2. THE TSI 1980/1990 COUNTER

At the VKI, information about TSI counters is available only in [5, 6].

2.1 Principle of operation

The counter type TSI signal processors measure the duration of a certain number of doppler periods (or cycles) in a doppler burst. In an input conditioner the doppler signal is band-pass filtered to suppress the pedestal and to reduce the noise, and then amplified; time envelopes based on the doppler cycles are generated. A timer measures the envelopes, validates the measurement and provides a digital output.

The **Input conditioner** (IC) features a two-level detection scheme. A zero-crossing detector yields a square wave based on zero-crossings following a rise above an hysteresis level; a pulse train is generated at the doppler frequency. A threshold detector selects the pulses corresponding to a signal level above a threshold. The IC creates time envelopes of different lengths starting at the first zero-crossing occurring after the signal has exceeded both hysteresis and threshold levels. The IC generates an end-of-burst (EOB) signal starting at the first zero-crossing occurring when the hysteresis is exceeded but not the threshold. The IC also performs the cycle-count on the pulse train.

The **Timer** determines the length of the envelopes. Which envelopes are processed depends on the operating mode selected. The timer performs validation if required. The data are latched to the output data buffer; the digital output consists of a 8-bit number of doppler cycles and a time (12-bit mantissa plus 4-bit exponent). Data ready and reset pulses are issued.

The 1980 model processes up to 100 MHz signals with 2 ns resolution, the 1990 up to 200 MHz with 1 ns resolution.

2.2 Modes of operation

The TSI counters can be operated in several modes depending on different signal processing features.

- The number of doppler cycles timed to measure the period is either a number preset by the operator, or the total number of cycles in the doppler burst that exceed the threshold level.
- The number of cycles delivered at the output is either the preset number used for timing, or the number of cycles above threshold.
- Validation is implemented or not.
- System reset, allowing a new measurement to be started, is performed before the end

of the burst or not.

The resulting modes are the total burst mode, the N-cycle mode (or comparison mode), and the single measurement per burst mode. Abbreviations and symbols are defined in the front tables.

2.2.1 Total Burst (TB) mode

In this mode the number N_t of cycles timed to measure the doppler period T_D is the number N_{tr} of cycles above threshold; the corresponding time T_{tr} is a measure of the length of the burst.

No validation is performed.

The reset pulse is issued after the EOB; only one measurement per burst is allowed.

The TB mode is selected by displaying red numbers m on the "Minimum Cycles/Burst" thumb-wheel switch. Signals are processed only if the number of cycles exceeds N_m :

$N_m = 2^m$ $\qquad$ (m = 1 to 4).

Digital Output (Fig. 2a) :

N: The number N_t of timed cycles $\qquad$ $N = N_t = N_{tr} \neq N_m$

T: The time corresponding to N_{tr} cycles $\qquad$ $T = T_{tr} = N_{tr} T_D$

2.2.2 N-cycle (NC) mode

In the N-cycle mode, which is most commonly used, the operator defines a number N_m of preset cycles which is a power of 2 :

$N_m = 2^m$ $\qquad$ (1980: m = 1 to 5; 1990: m = 1 to 7)

The number N_t of cycles timed to measure the doppler period T_D is N_m.

It is possible to perform validation by comparing the time envelope for N_m cycles to twice the envelope for $N_m/2$ cycles.

Once the envelope timed and validated, data are transferred to the output data buffer and a reset pulse is issued immediately. A new measurement may be completed on the same doppler burst provided the total number of cycles is large enough and the computation time is short with respect to the duration of the burst.

Neither the number of cycles above threshold nor the burst duration are measured.

The NC mode is selected by displaying white numbers m on the thumb-wheel switch.

Digital Output (Fig. 2b) :

N: The number N_t of timed cycles $\qquad N = N_t = N_m$

T: The time corresponding to N_m cycles $\qquad T = T_m = N_m T_D$

2.2.3 Single Measurement per Burst (SMB) mode

This mode is derived from the N-cycle mode by requiring that the reset pulse should not be issued before the EOB. Only one measurement per burst is allowed. The SMB mode can be selected on any TSI counter by grounding pin 11 on the digital output connector (§C.2), white numbers being displayed on the thumb-wheel switch.

If the serial number of the counter is less than 500, there is no other modification. The digital output is the same as in the N-cycle mode and no information on the burst length is available.

If the serial number is 500 or up (Appendix A of [5]), the number of cycles at the output is also modified. Instead of N_t, the number N_{tr} above threshold is made available, from which the length of the burst $T_{tr} = N_{tr} T_D$ can be obtained. Note that nothing is changed on the period timing or on the validation procedure; validation is performed only on the N_t timed cycles used to measure the doppler period T_D, and not on the following cycles. An error occurring in counting the latter is not detected and affects the total number of cycles counted N_{tr}, even if the period measurement is validated.

Digital Output (Fig. 2c) :

N: The number N_{tr} of cycles above threshold $\qquad N = N_{tr} \neq N_t = N_m$

T: The time corresponding to N_m cycles $\qquad T = T_m = N_m T_D$

2.3 Selection of operating mode

When it is simultaneously required :

- to allow only one measurement per burst,
- to get a measure of burst duration,
- to have data validation,

the only way is to operate a counter with serial number above 500 in the single measurement per burst mode.

2.4 The data rate

The maximum rate at which measurements can be performed and data made available at the output of the processor, is determined by the time elapsed between the beginning of the time envelopes and the system reset. This time is made up from a time envelope and a dead time. The time envelope is the longest envelope NT_D created by the processor, i.e, T_{tr} in TB and SMB modes, and T_m in the NC mode. The dead time includes the time required to measure the envelope ($=T_D$), to make the comparison for data validation (1.25 μs) and to shift data to the output (0.9 (LF) to 2.6 μs (HF)). In the SMB mode the envelope and the dead time may overlap, because envelope measurement and comparison start after N_m cycles (Fig. 2c). At low doppler frequency, the comparison and output update times are negligible and the time practically reduces to $(N+1)T_D$, which is the situation illustrated in Fig. 2. At high doppler frequency the dead time becomes predominant and reduces the maximum data rate.

3. MEASUREMENTS

3.1 Apparatus

3.1.1 Doppler signals

Tests of operation of the TSI counters are performed using artificial doppler signals produced by function generators. The basis of the different kinds of signals is a sinusoidal carrier at doppler frequency. Four kinds of amplitude modulation (AM) are used :
A : No amplitude modulation,
B : Sinusoidal amplitude modulation,
C : Sinusoidal amplitude modulation with pedestal,
D : Gaussian-shaped modulation.

Type B (Fig. 3a) signals are obtained by driving a PM5134 Philips function generator in the X-TAL AM mode; the modulation signal, applied at the rear AM-INPUT, is provided by a second generator (Wavetek 180 or IEC F34). The modulation depth is determined by the level of the modulation signal. When this level is increased above the value corresponding to 100% modulation depth, the bursts in the AM signal are separated by flat parts (null voltage); the duration of the burst is shorter than the period of the modulation signal (Fig. 3b).

Type C (Fig. 3c) signals are produced by feeding a carrier from a PM5134 function generator into a Doppler Signal Simulator (DSS)* which provides equally spaced bursts with pedestals. A short description of the DSS, built by Timmerman [7], and an operating procedure are given in Appendix A.

Type D (Fig. 3d) signals are produced by a PM5138 Philips function generator, programmable by a microcomputer via an IEEE 488 interface. Waveform generation is described in Appendix B.

The following terminology is adopted :
the **doppler frequency** is the high frequency or carrier frequency,
the **modulation frequency**, which determines burst occurrence, is the low frequency,
the **modulation ratio (MR)** is the ratio of doppler to modulation frequency,
the **burst presence ratio (BPR)** is the ratio of the burst length (flat part excluded) to the modulation period.
The number of cycles in a burst is equal to the product of the burst presence ratio and the modulation ratio.

The characteristics of the signals used for the tests are the following (L: lower limit; H: higher limit) :

---

* obtained from the Ecole Royale Militaire, by courtesy of Professor R. Decuypere

Doppler frequency :

L : 1 kHz, fixed by the processor;

H : fixed by the generator : PM5134 : 20 MHz; PM5138 : practically 2 MHz, because at least ten samples per doppler cycle are required to obtain correct signals, 40 samples (500 kHz) being required in some cases.

Modulation ratio :

fixed by the processor; L : N_m; H : 256, capacity of the cycle-counting 8-bit register.

Burst presence ratio :

Type B signals : 70-100%; type C : 50%; type D : $\leq 100\%$.

Signal levels were measured on a dual-trace Philips PM3215 50 MHz oscilloscope with 10 MΩ inputs.

3.1.2 TSI counters

In order to be able to distinguish between possible malfunctions and inherent insufficiencies, measurements were performed with two counters.
VKI Counter : TSI 1990A, Serial number 520.
ERM Counter* : TSI 1980, Serial number 277.

3.1.3 Data acquisition system (DAS)

Digital data from the TSI counter are read by a Commodore CBM 8032 and a VKI CEI, and stored in CBM memory. Once the acquisition completed, data are transferred on cassette tape to be processed on the VAX cluster. The DAS (Fig. 4) is described in Appendix C.

3.2 Measuring the threshold detector level

The value of the threshold is estimated by measuring the peak-to-peak (pp) level of the filtered signal required to light on permanently the green indicator:
TSI 1980 92 mV (pp). (NC and TB modes).
TSI 1990A 116 mV (pp). (NC, TB and SMB modes).

These figures are independent of the cycle/burst setting N_m. It is worth noting that the level at which the counter starts operating (non-zero data rate) is higher than 116 mV(pp) for $m > 3$ in the TB and SMB modes on the 1990A; (not measured on the 1980).

There is a good agreement with the threshold value quoted in the manual [5] : amplitude 50 mV, i.e., 100 mV(pp). Whether the threshold can be adjusted by the operator (e.g. on an internal potentiometer) is not known.

---

* obtained from the Ecole Royale Militaire, by courtesy of Professor R. Decuypere

Operating conditions :
Inputs : NC mode: Type A signals, 100 kHz, 1 V (pp).
TB and SMB modes : Type B signals, 1 V(pp), 100 kHz modulated by 1 kHz.
Settings : Filters OFF, Comparison 0%.

3.3 Test of the cycle-counting function

In order to point out the influence of the threshold detector level on the cycle-counting function, the number of doppler periods measured by the counter is recorded as a function of the filtered signal level. A constant input level is fed into the PHOTO-DET input; the level of the filtered signal is varied by modifying the gain in the range where the green light is on; the peak-to-peak value is measured on the scope.

Inputs :
Type B signals: 1 V; unless otherwise specified.

Type C signals are produced with 3.4 V at the output of the HF generator, unless otherwise specified. The VKI amplifier (gain=35, §A.4) is always used between the DSS and the TSI processor. Typical values of the doppler signal level and visibility at DSS output with load (amplifier and processor), depend on the doppler frequency (MR=40): 10 kHz 76 mV, 45%; 1 MHz 48 mV, 78%; 20 MHz 34 mV, 30%.

Type D signals: 1 V, unless otherwise specified.

Settings :
Amplitude limit OFF; Comparison 7% (SMB mode), 0% (TB mode).
Minimum cycles/Burst, SMB mode, N_m=8, unless otherwise specified.
Filters: Type B signals: OFF;
Type C signals are high-pass filtered with the highest LO-LIMIT smaller than the doppler frequency.
Type D signals are band-pass filtered; the HI-LIMIT is always lower than the sampling rate of the PM5138 generator, so that the influence of digitization on signal shape is smoothed away.

3.3.1 Dependence on signal level

Doppler frequencies below or equal to 2 MHz. The number of cycles actually measured is plotted (Fig. 5) as a function of the filtered signal level of the 1990A (SMB and TB modes) and 1980 (TB mode). Type B signals with approx 80% BPR are used; the modulation ratio is 100, each burst containing about 80 cycles. The percentage of measured periods refers, however, to the modulation ratio (100), and not to the number of cycles in the burst, which cannot be accurately determined. Signal levels range from 100-150 mV to 1.5 V(pp); at 1.5 V nearly all cycles are counted; close to the threshold very

few cycles are counted. The number of cycles depends strongly on the signal level. Data corresponding to different doppler frequencies fit a single curve. In these conditions the cycle-counting process depends only on the ratio of signal to threshold level in agreement with the description of §1.4. If one requires more cycles to be counted before validation, only signals with higher levels are processed. For instance, if N_m=64 cycles are required (Fig. 9a), instead of 8 (Fig. 5a), only signals higher than 500 mV are processed.

Similar measurements were also performed in the same conditions with a modulation ratio of 25 (80% BPR), by changing the modulation frequency. Results (Fig. 6) show that the single curve fit is obeyed only up to 500 mV (1990A) or even 250 mV (1980); at higher levels erratic values are obtained; percentages above 80%, physically impossible in a single burst, are found in figures 6a and 6c *.

Doppler frequencies above 2 MHz. Above 2 MHz (Fig. 7) (MR=100, BPR=80%), the behaviour is quite different. The upper and lower limits of the signal range, as measured by the scope, get smaller and smaller. At 20 MHz the range is 30-400 mV(pp). This is caused by the HF attenuation in the cables and circuits; the voltage sensed by the scope is not the same as that sensed by the threshold detector. This explains why, compared to LF curves, HF data are obtained at lower voltages. All 5 MHz curves, the 10 MHz curve (Fig. 7b) may be considered as simply shifted towards lower voltages. The 20 MHz response is on the other hand almost completely flat; the number of cycles, different in the SMB and TB modes, is unexpected. The 10 MHz curve (Figs. 7a and 7c) exhibit a flat part above 200 mV, the number of cycles being lower than expected.

With a modulation ratio of 25, figure 8 shows examples of any kind of behaviour:
merely shifted curve: 20 MHz Fig.8a,
flat response: 5 MHz (Fig. 8b), 10 MHz (Fig. 8a), 20 MHz (Fig. 8c),
partially flat curve: 20 MHz (Fig. 8b),
erratic counts at high voltage levels: 5 and 10 MHz (Fig.8c).
It is striking that changing the modulation ratio totally modifies the kind of response: compare the 20 MHz response in figures 7a and 8a in the SMB mode, or the 5 MHz response in figures 7b and 8b in the TB mode. So does also switching from SMB to TB modes, compare figures 7a and 7b, or 8a and 8b. Even the response of each processor in identical conditions may be totally different (Figs. 8a and 8b).

High- and low-counts. The preceding results show that wrong values of the number of counted cycles are measured. High values, sometimes physically impossible, are met only at the lower modulation ratio; they will be referred to as **high-counts**; their occurrence is discussed in §3.3.2. Low values, occurring mostly above 2 MHz will be referred to as **low-counts**, and discussed in §3.3.3.

---

* In this figure, values above 100% are reduced to 100%.

3.3.2 Interpretation of high-counts

Counting over several bursts. The fact that counts higher than the number of cycles in a burst are recorded can be understood if the counter keeps counting from a burst to the following. This is confirmed by histograms of counts. In type B signals with MR=25 and BPR=80%, 20 cycles are theoretically found in each burst. Besides expected values of 19-20 cycles, figure 13a clearly shows high-counts at 39-40 cycles (2 bursts) and 59-60 (3 bursts). The EOB detection fails in this case, so that counts are totalized over several bursts.

High-counts were recorded with a modulation ratio of 25, but never of 100. Histograms confirm the interpretation of high-counts produced by the 1990A up to 1 MHz at 1500 mV(pp) in the SMB mode (Fig. 6a), and at 100 kHz (1200 mV) in the TB mode (Fig. 6b). In the case of the 1980 (TB mode, Fig. 6c*), the same interpretation is valid for all high-counts occurring at 1 and 1.5 V (10 kHz-2 MHz), as well as at 0.5 and 0.75 V (2 MHz).

The failure of the EOB detection. The reason of EOB detection failure is found in the shape of the test signals. The generation of the EOB signal (§2.1) occurs if:

1. the hysteresis level** is exceeded,
2. the threshold level (§3.2) is not exceeded.

High-counts were first observed in experiments with type B signals without separation between bursts (Fig. 3a, BPR=100%), corresponding to 100% modulation depth. It is, however, difficult to adjust on the scope screen the modulation depth at exactly 100% via the level of the modulation signal. When the modulation depth is set accidentally below 100%, the height of the smallest peak, at the junction of the bursts, may be still above the threshold (Fig. 14a), violating condition 2. This is only likely with high level signals containing few cycles; these are precisely the conditions of high-count occurrence. To avoid accidental modulation depth less than 100%, the level of the modulation signal was increased above the 100% level. In this way, flat parts up to 20% of the modulation period are introduced (Fig. 3b, BPR=80%). Experiments reported in figure 6 (type B signals, BPR=80%) yielded nevertheless high-counts. In experiments with type C signals (50% flat parts), high-counts are again observed (Figs. 10 and 11). The modulation ratio is chosen equal to 40 to keep the same number of cycles (20) as with type B signals of MR=25 ($40\times0.50=25\times0.80$). Histograms confirm the interpretation of high-counts occurring either in the SMB mode (Fig. 10a) at 1 MHz (0.75 and 1 V) or 2 MHz (0.75 V) as well as in the TB mode (Fig. 10b) at 10 kHz (0.5 and 0.75 V), 100 kHz (1 V), or (Fig. 11b) at 5 MHz

---

* In this figure, values above 100% are reduced to 100%

** The nominal hysteresis level is 10 mV *not pp* [5], but the actual level was not measured

(0.3 V) and 20 MHz (0.3 V). The use of type C signals does not suppress high-counts occurrence.

The length of the flat part is probably not important because condition 1. must also be satisfied, i.e., a doppler peak must be found between hysteresis and threshold levels. The edges of the signals used (B, or C) are quite abrupt, so that it is possible that no doppler peak occurs between these levels (Fig. 14b); no EOB signal is generated and the processor goes on counting on the next burst; the process is sometimes cumulative. This interpretation is fully compatible with the fact that signals with a large number of cycles never produce a high-count; there is always at least one peak between the levels. For the same reason high-counts occur only at high signal levels.

It seems reasonable to ascribe the occurrence of high-counts to the peculiarities of test signals. Appropriate test signals for LDV must have slowly varying edges to generate reliable end-of-bursts. This hypothesis can be tested with gaussian-shaped type D signals. Gaussian signals (Fig. 14c) have much smoother edges than sinusoidal ones. It is unlikely that no peak could be found between hysteresis and threshold levels. The fact that EOB failure can be simulated on computer generated signal shapes (Fig. 14) strongly supports this interpretation.

Verification with type D signals. Tests were performed on the 1990A in the SMB and TB modes.

Type D signals with MR=25 are generated with BPR=80 and 100%. No frequencies higher than 2 MHz are used because the number of samples per cycle would have been too small. Signals at 2 MHz, generated with $NBURST$=4 (§B.2) are digitized by only 10 samples per cycle and are more irregular than 1 MHz ($NBURST$=2, 20 samples) or lower frequency signals ($NBURST$=1, 40 samples). The irregularity is clearly seen on the scope because the sequence of peak amplitudes is not smoothly varying. The differences in signal generation are the only reason why 1 and 2 MHz measurements fall slightly above others (Fig. 12). The discrepancy amounts to only one cycle. Histograms confirm in every case that high-counts, involving more than one burst are never encountered. The smoothness of the edges avoids any counts over several bursts, even with contiguous signals without flat parts (BPR=100%).

Type D signals with MR=100 are also generated with BPR=80 and 100% in the SMB mode. Band-passed signals up to 2 MHz are generated in only one way, ($NBURST$=1, 10 samples per cycle). Measurements (Fig. 12c) collapse very nicely on a single curve. No high-counts are observed, just like in the case of type B signals.

No doubt is left that the origin of the high-counts detected must be totally ascribed to the failure of the end-of-burst detection on signals with steep edges, because no peak is found between hysteresis and threshold levels.

3.3.3 Interpretation of low-counts.

Low-count occurrence. The occurrence of low-counts was detected very soon in an experiment performed to check whether the number of measured cycles was independent of the doppler frequency or not. The selected test conditions, type B signals, MR=100, without particular attention to the BPR ($\approx$ 100%) or to the level of the signal, showed (Fig. 15) a decrease above 5 MHz. The regularity of this behaviour was indeed puzzling, and it took a lot of time and efforts, involving tests with type D signals and also with another processor*, to identify the relevant parameter.

Histograms (Fig. 13b) show that low values of the percentage of measured cycles occur because low cycle-counts (9-10) are recorded in addition to correct ones (18-19 cycles). Low-counts were recorded with both processors, in the SMB and TB modes, with type B (Figs. 6, 7, 8), type C (Fig. 10) and type D signals (Fig. 12b: 1 V, 2 MHz). They were recorded mainly, but not exclusively, at doppler frequencies above 2 MHz and at high signal level. It was already noted in §3.3.1 that changing the modulation ratio or switching the operation mode modifies completely the response of the processor; the 1990A and 1980 processors do not behave in the same way in presence of the same signals measured in the same conditions.

The phenomenon depends also on the number of cycles required for validation. Signals containing 80 cycles (MR=100, BPR=80%), processed in the SMB mode with N_m=8 cycles, show a flat response of low-counts (Fig. 7a); the percentage of measured cycles is about 63% at 10 MHz and 23% at 20 MHz; in both cases less than 64 cycles are counted. If the same signals are processed with N_m=64 cycles (Fig. 9b), low-counts are still observed at 10 MHz, but the percentage is raised to 67%, slightly above N_m; at 20 MHz low-counts disappear, the response is similar to the 5 MHz normal response, taking into account the voltage shift due to HF attenuation (§3.3.1).

The relevant parameter. The clue was found by carefully recording the number of cycles together with the data rate** at constant doppler frequency and variable modulation ratio. At 20 MHz, figure 16a shows that starting at high MR from an expected value of 74%, the percentage regularly decreases, then suddenly recovers the original value, up to four times. At 10 MHz (Fig. 17a) the second and further drops are less regular. It is clearly seen that the data rate of the processor is involved by plotting the ratio of the data rate to the maximum theoretical rate, which is the burst rate, i.e., the modulation frequency. Starting from high MR (Fig. 16b), after each drop of the percentage of cycles, the relative data rate falls respectively to 1/2, 1/3, 1/4 and 1/5 of the maximum rate, showing that only every $2^{nd}, 3^{rd}, 4^{th}$ or 5^{th} burst is measured.

---

* Phase Doppler Particle Analyser (PDPA), Aerometrics.

** displayed on the front panel of the 1992 readout module

The limiting factor is the data rate of the processor. The data rate was measured with sinusoidal (type A) signals in the NC mode with N_m=8, as a function of doppler frequency (Fig. 18). This is a "free-wheeling" rate ν_f because in these conditions, no EOB signal is required, the reset immediately follows the validation, and a new measurement can be initiated on the sine wave. The values at 20 and 10 MHz are respectively 235 and 222 kHz. The vertical lines in figures 16b and 17b are drawn at modulation frequencies respectively equal to ν_f, $\nu_f/2$, $\nu_f/3$ and $\nu_f/4$. At 20 MHz the drops in the plots are closely predicted by the lines; at 10 MHz, the correspondence is slightly worse, but undoubtedly sufficient to prove the relevance of the data rate.

Explanation of low-counts. At high modulation ratio the burst rate is low; the processor validates, updates the output and issues the reset pulse during the time the signal is less than the threshold level. The measurement on the second burst starts at the right time and a correct number of cycles is measured. As the MR is reduced, the time between consecutive bursts decreases and, when the processor gets ready on the second burst, the threshold level is already overshot; a few cycles are lost and the number of measured cycles is too low. When the MR is further reduced, the number of cycles falls to a value close to N_m, below which no measurement is possible; the second burst is skipped and a correct count is performed on the third burst, restoring the correct number of cycles. As successively 1, 2, 3, or 4 bursts are skipped, the data rate falls to 1/2, 1/3, 1/4 or 1/5 of the burst rate.

The explanation is fully compatible with the fact that low-counts occur mainly at high signal level (cycles are counted over the entire burst), or at high doppler frequencies (the dead time is predominant); and also with differences between SMB and TB modes (at 20 MHz the comparison time lasts 25 cycles). The difference between 1980 and 1990A processors is not understood, because their data rate is in principle identical [6]. The above difference between measurements with N_m=8 (Fig. 7a) and N_m=64 (Fig. 9b) (modulation frequency 200 kHz) is easily explained. With N_m=8 the data rate is 200 kHz, only 23 cycles are measured, but on every burst. With N_m=64 the data rate is only 100 kHz, the correct number of cycles (function of signal level) is measured, but only on every second burst.

Combined dead time effect and EOB failure were also observed in the TB mode in signals containing few cycles. If the dead time causes the cycle-count to start late in a burst (low-count), at the end of the burst less than N_m cycles are counted; either the EOB operates and the measurement is rejected, or it does not and the following burst is also counted. Cycle-counts corresponding to approx 1 1/2, 2 1/2 ... bursts were actually recorded. In the SMB mode, doppler period validation reject these counts.

From figures 16b and 17b it can be concluded that the risk of low-counts begins when the burst rate (modulation frequency) rises to about 75 kHz, which is 1/3 of the free-wheeling rate for signals processed with N_m=8. Actually, provided good signals are used,

low-counts are hardly observed below 80 kHz. Never with correctly filtered type D signals; once (1990A, TB, MR=25) with type B signals at 40 kHz; several times (1990A/SMB, 1980/TB, MR=40) with type C signals at 50 and 25 kHz. But with incorrectly filtered (HI-LIMIT equal to the sampling rate of the PM5138, §3.3) type D signals (1990A, SMB, MR=100), low-counts are observed at any burst rate (10 Hz to 20 kHz). At such rates any role of the dead time is excluded; occurrence of premature EOB due to irregular signal shape is likely, but has not been proved.

Prevention of low-counts. The most important consideration is that such high burst rates, due to the contiguous character of the bursts in the test signals, are artificial. In low-speed flows, provided the signal presence percentage is low (individual realization conditions), the probability that the dead time extends over some part of the next signal is small. It is worth noting that the signal presence percentage *must* be kept low in order to avoid errors on the measurement of burst duration; such errors are possible even if the corresponding velocity is correctly measured because the latter is measured and validated over a preset number of N_m cycles (§2.2.3). Like in the case of the high-counts the source of the trouble is found in the nature of the test signals.

3.4 Accuracy of frequency measurements

SMB mode (1990A). Frequency measurements are done by counting a fixed number of cycles ($N_t = N_m$); the validation of individual counts is performed in this experiment with 7% comparison between N_m and $N_m/2$ time envelopes. With type B signals the accuracy of the mean frequency (255 samples) is always better than 0.1% up to doppler frequencies of 2 MHz, but slightly worse at higher frequencies; values up to 0.5% are found at 20 MHz in signals containing 20 cycles. With type C signals (20 cycles), very distorted at high pedestal frequencies (§A.2), the accuracy is better than 0.1% up to pedestal frequencies of 25 kHz, 0.5% at 50 kHz and a few percent above; the worse accuracy (5%) was observed once at 250 kHz. With type D signals (doppler frequency less than 2 MHz), the accuracy is better than 0.1% with properly filtered signals and 0.2% in any other case. In the SMB mode the mean frequency is correctly estimated within the preset comparison limits, even if cycle-counts are wrong, whether high- or low-counts.

TB mode. Frequency measurements are made on the total number of cycles counted ($N_t = N_{tr}$); no validation is performed. At high modulation ratio (type B signals containing 80 cycles), no EOB failure occurs and only low-counts caused by the dead time of the processor are observed (above 10 MHz); frequency measurements are correct and the accuracy is found in the same limits as in the SMB mode.

At lower modulation ratio (signals containing only 20 cycles), the situation is more complex. The calculated mean frequency is either correct or lower than the carrier frequency. When the EOB fails, too low frequencies are always measured because the time between two bursts is included in the period timing envelope. It is, however, possible to

prove EOB failure occurrence only when the number of counted cycles is larger than the nominal number of cycles of the burst (high-count). In the opposite case, it is not possible to prove that the incorrect frequency result is caused by an EOB failure. The fact that with correctly generated (40 samples/cycle) type D signals, neither EOB failure nor incorrect frequencies are met is nevertheless a strong argument in favour of such a causality link; the accuracy is found better than 0.3% up to doppler frequencies of 500 kHz.

With type B signals, errors up to 12% on the mean frequency are obtained at any frequency with the highest signal levels (the upper half-range). With type C signals (1980), the situation is even worse; errors up to 65% are measured in the upper half-range (pedestal frequency up to 50 kHz), or in the whole range (above 50 kHz). With type D gaussian signals (1990A) at 1 MHz, signals are digitized into a small number of samples and yield too low frequencies (errors up to 50%); at 2 MHz, errors up to 5% are registered.

In the TB mode correct frequency measurements are obtained only with good quality signals, in the absence of EOB failure.

4. DISCUSSION

4.1 The cycle-counting function

4.1.1 Dependence on signal level

Measurements have confirmed that the number of cycles counted in a doppler burst by TSI counters depends on the level of the signal in the way predicted (§1.4) by the comparison of signal level to a fixed threshold. At low signal level, the variation is important but becomes negligible at high levels, practically above 500 mV (Fig. 5). It does not seem possible to get rid of this dependence and to obtain transit time measurements unaffected by the level of the signal :

- It is unlikely that LDV measurements could be performed in such conditions that only high level signals are produced and processed, because in these conditions the SNR would be too low.
- Selecting only the few highest signals by amplitude discrimination would be the source of errors because such signals are likely to arise from large particles which do not follow the flow.
- The number of counted cycles varies much less (Fig. 9) when the minimum number of cycles N_m required to process a signal is not small with respect to the number of cycles in the burst. But this practice would select particles whose major velocity component is perpendicular to the fringe planes, and introduce a directional bias.

In the case of the TSI counter processor, transit time weighting will anyway require to average out on a very large number of samples the dispersion introduced by the effect of signal level. The possibility of overcoming the difficulty with LDV processors featuring other detection or operation principles must be examined :

Frequency domain processors. FFT based processors are much less sensitive to noise than zero-crossings based timing processors. This opens an opportunity to process high-level signals in order to obtain level independent burst timing, even with fixed threshold detection.

Logarithmic signal amplification. The selective amplification of low-level signals lowers the detection threshold of photomultiplier signals, and flattens the response of the cycle-counting function to the level of the signal. But this response is corrected only in part, because a steep rise of the number of measured cycles still occurs in the lower signal range, where the SNR is acceptable. This point has been confirmed by measurements performed with the PDPA processor (Aerometrics).

Burst length definition by relative levels. The most promising solution must be found in separating the measurement of the burst length from the measurement of the

doppler frequency. It is then possible to time a burst envelope by measuring the time elapsed between relative envelope levels.

4.1.2 End-of-burst failure

Several cases of wrong cycle-counts have been observed. High-counts occur with high-level signals containing few cycles (low modulation ratio), when the edges are very steep (type B and C signals). In the SMB mode, the frequency is always correct but the cycle-count is wrong; in the TB mode both are wrong. High-counts are produced when the end-of-burst function fails to detect the end of the signal, so that the processor goes on counting during the following burst. All high-counts are caused by the shape of the bursts in the test signals. This phenomenon is totally excluded with gaussian signals in actual measurements.

The same kind of error will occur with the TSI counter in actual measurements when doppler bursts overlap (Fig. 19a); the period measurement is validated on the first burst while cycles are totalized on both. There is a lack of a rejection system which avoids extending burst length measurements on overlapping bursts. Safe measurements will be obtained only at such particle rates that the signal presence percentage is low and the probability of overlapping bursts is negligible.

4.1.3 Effect of the burst rate

Low-counts occur mainly with high-level signals, whatever the number of cycles, as soon as the burst rate is high. In any mode the cycle-count is wrong but the frequency is correct, provided in addition no end-of-burst failure occurs. Systematic low-counts are produced when the repetition frequency of contiguous signals is so high that the dead time of the processor spreads over a significant part of the following burst (Fig. 19b); the cycle-counting starts too late but the end-of-burst occurs correctly. The possibility of generating non-contiguous signals by externally triggering the PM5138 generator in the burst mode under computer control has been considered; low burst rates without dead time effect can be obtained. The realization has not been undertaken because of the GPIB transmission problems quoted in §B.3.

In actual measurements this phenomenon can be avoided only if the signal presence percentage is, again, low and the probability of finding closely following bursts is negligible. A rejection logic should avoid starting burst length measurements in the middle of a burst.

Other cases of low-counts have also been observed at such low doppler and repetition frequencies that any role of the dead time is excluded. Occurrence of premature end-of-burst is likely in this case, but has not been proved. The influence of bad signal shape has been put in evidence in some cases. Such errors were found more frequent by processing high level signals. In actual measurements wrong cycle-counts cannot therefore

be excluded, and, because no validation is performed on cycle-counting, will introduce an error in transit time weighting.

4.1.4 Definition of a suitable processor

A suitable processor for transit time weighting should involve:

- Transit time measurements independent of signal level.
- Implementation of some rejection system to avoid measuring transit times on overlapping bursts.
- Implementation of some rejection system to avoid starting transit time in the middle of a burst.
- In the case of transit time measurements by cycle-counting, a cycle-counting register capable of accommodating the large number of cycles obtained with slow particles in the case of frequency shifting.

4.2 The generation of doppler signals

4.2.1 Test signals used in this investigation

The test signals used in this investigation differ from actual signals in many aspects:

- They have no pedestal, except type C signals.
- They are not gaussian-shaped, except type D signals.
- The occurrence of signals is repetitive, regular instead of random; the bursts are contiguous (BPR=100%), or nearly (BPR$\geq$50%).
- High frequency signals, above a few MHz, are somewhat distorted.

The absence of pedestal has never been a problem, because the pedestal is filtered out before processing.

Non-gaussian signals were found to exhibit too steep edges causing failure of the end-of-burst detection in high level signals containing few cycles; incorrect cycle-counts are obtained in SMB and TB modes, but frequency measurements are correct in the former mode.

Due to the contiguous character of the signals, the dead time of the processor interferes with cycle-counting on the following burst. Incorrect cycle-counts are obtained in SMB and TB modes, but frequency measurements are nevertheless correct.

Distortion at high frequency is caused by the generator. The PM5134 generates asymmetry between positive and negative half-waves, while some residual ripple is found on the flat parts between bursts; this may be related to the fact that the maximum external modulation capacity of the PM5134 is nominally 20 kHz. With the DSS similar difficulties were noted with pedestal frequencies above 50 kHz (§3.4). On the PM5138 the limitation is found in the sampling rate (≈20 MHz); the digitization of high-frequency doppler cycles is made with too few points, and a regular variation of peak amplitudes is no longer obtained.

The possibility of testing LDV processors by so simple signals as repetitive amplitude modulated sinusoidal signals from function generators was of course a priori questionable. For this reason the Doppler Signal Simulator DSS was welcome as an alternative. But the fact that the same problem has been met with both kinds of signal generators was unexpected, and for a long time misleading, because too much attention was paid to processor operation instead of signal definition.

4.2.2 Definition of a proper doppler generator

A doppler signal generator should meet the following requirements:

- The edges of the bursts must be gaussian-shaped, or at least slowly decaying.
- Undistorted signal must be generated in the HF range corresponding to the particular application; the range of signals obtained with frequency shifting by Bragg cells at 40 MHz must anyway be included.
- The repetition rate of the bursts must be much lower than the maximum data rate of the processor at the given doppler frequency.

Fulfilling these requirements will allow to test safely the doppler period timing and cycle-counting functions. As long as the visibility of the signals is not relevant, it is not necessary to simulate complete signals with pedestals; testing the high-pass filter can be performed by other means. The possibility of randomly triggering the arrival of the bursts on the processor, following e.g. a Poisson distribution, must be mentioned. This provides a tool to study the errors introduced by particle arrival statistics on single realization measurements [1].

5. CONCLUSIONS

It is shown that the number of cycles counted in a doppler burst strongly depends on the ratio of signal to threshold detector level in a quite predictable way. The variation is very important in the low-level signal range which is more likely to be used because of SNR requirements. A logarithmic amplifier does not bring the solution of the problem, which is simply transferred towards lower signal levels. The cycle-counting process is proven independent of the doppler frequency; no bias will be introduced on weighted velocity measurements. Indirect accuracy limitations will unavoidably arise from the dispersion introduced on transit time measurements by the effect of signal level; the error introduced by this dispersion can be reduced only by processing a very large number of individual measurements. Transit time weighting with the TSI processor may be considered as valid, but its accuracy is questionable. The conditions that a processor must fulfill in order to measure correctly the transit time are defined.

None of the three kinds of signal generators was able to provide correct synthetic doppler signals in a suitable frequency range. Incorrect cycle-counts have been encountered because the signals used for test purposes were different from actual LDV signals. The first problem is caused by the occurrence of end-of-burst failure due to improper shape of signal modulation. Another problem is caused by the dead time of the processor when the rate of repetitive doppler bursts is no longer small with respect to the intrinsic data rate of the processor. In the case of user-defined waveform, it is necessary to define every doppler cycle by a large number of samples in order to generate correct signal shapes; only doppler frequencies much lower than the sampling rate of the generator can be practically generated. The necessity of making available a more performing doppler signal generator is demonstrated.

REFERENCES

1. Leprince, F. & Riethmuller, M.L.: Skin friction determination by LDV measurements in a viscous sublayer. Analysis of systematic errors. von Karman Institute TN 156, Dec. 1985.

2. George, W.K.: Limitations to measuring accuracy inherent in the laser doppler signal. Proceedings of the LDA-Symposium, Copenhagen 1975, pp 20-63.

3. Buchhave, P.; George, W.K.; Lumley, J.L.: The measurement of turbulence with the laser-doppler anemometer. Ann. Rev. Fluid Mech., Vol. 11, 1979, pp 443-503.

4. Petrie, H.L.; Samimy, M.; Addy, A.L.: An evaluation of LDV velocity and fringe bias effects in separated high speed turbulent flows. ICIASF '85 Record, pp 297-308.

5. Instruction Manual. Model 1990 Counter Type Signal Processor for Laser Velocimeter.

6. Laser Velocimetry Systems. TSI Incorporated. Form No. TSI LDV-879-23M-2M BRI.

7. Timmerman, M.: Optische simultane meting van de grootte en de snelheid van deeltjes in een stroming. Ph.D. Thesis Rijksuniversiteit Gent, Maart 1982.

APPENDIX A - DOPPLER SIGNAL SIMULATOR (DSS)

A.1 Description

The DSS cabinet includes two power supply modules, a DSS module, an Automatic Filter Unit module and an output section. A HF carrier (doppler frequency) from an external generator is fed to the HF INPUT. The DSS module produces repetitive bursts with a selectable pedestal frequency (modulation frequency). During the first half of the modulation period, a signal with pedestal is issued; a null voltage is maintained during the second half period; signals with 50% BPR are obtained. The edges of the burst are very sharply defined.

A.2 Selection of pedestal frequency

This version of the DSS differs from that described in [5] where the ratio of carrier to pedestal frequency is fixed to 20. The pedestal frequency can be adjusted by the FREQ and FREQ FINE knobs. The FREQ knob has 9 positions, 4 of which are labeled 10k-100k-1M-10M. The pedestal frequencies corresponding to the 9 positions were measured by means of the scope in the extreme positions of the FREQ FINE control : (CW : fully clockwise; CCW : fully counterclockwise).

		CCW	CW	
1	10 k	150 Hz	1850 Hz	
2	-	300	3850	
3	100k	1400	17.9 kHz	
4	-	2560	32.3	
5	1M	15.2 kHz	179	
6	-	22.7	263	
7	10 M	70.4	641	signal distorted
8	-	90.9	769	signal distorted
9	-	152	1.11 MHz	very distorted

Note that the signal is less distorted in intermediate positions of the FREQ FINE knob.

A.3 Selection of signal visibility

The visibility of the signal increases with the output level of the HF generator. Visibilities above a certain value cannot be obtained, because a further increase of the generator output level obliterates the signal by introducing waves in the flat parts between bursts.

Both signal level and visibility are modified when the DSS output is connected to the TSI input. Signal level and visibility at DSS output are found to depend strongly on the doppler frequency.

A.4 Operating procedure

1 Set ON power switch at rear of cabinet.

2 Pedestal

a) Turn AMPLITUDE knob fully clockwise; display output on scope screen; the amplitude of the pedestal signal is 54 mV.

b) With aid of the time base of the scope, set pedestal frequency by adjusting FREQ and FREQ FINE knobs.

3 Doppler signal

a) Set doppler frequency on HF generator; adjust HF generator output level to approx 1 V(pp)*; connect generator output to HF INPUT.

b) Display OUTPUT on scope screen; each burst contains a number of cycles roughly equal to half the ratio of doppler to pedestal frequency.

c) Set signal visibility by adjusting the HF generator output level.

4 Feeding the TSI processor

a) Connect OUTPUT to PHOTO-DET input of TSI. Set LO LIMIT and HI LIMIT filters OFF. Display FILTERED OUT output on scope screen. The signal is distorted by low frequencies. Bring LO LIMIT at highest value below doppler frequency. This ensures highest filtered signal without distortion.

b) The level of the filtered signal can be adjusted:
-by the gain control on the TSI processor,
-by varying the amplitude of the output of the HF generator; in this way, the visibility of the signal is also modified.
The maximum level obtained on the TSI 1980 is about 700 mV; on the TSI 1990A about 600 mV.

c) Higher levels can be obtained by putting an amplifier between the DSS and the TSI processor:

---

* Levels are measured with a direct connection to the 1 MΩ scope input, without any connection to the HF input of the DSS.

TSI 10099 1 kHz-200 MHz, Gain=5

VKI 10 kHz* -50 MHz, Gain=35

The latter introduces a small LF distortion for the lowest pedestal frequencies, without any influence on the filtered signal.

* The lower limit was later modified to 0.2 kHz.

37-Pin male connector.

	Pin
Ground	1
N0	2
N3	3
N1	4
N2	5
N6	6
N7	7
N5	8
N4	9
Data Inhibit	10
SMB	11
	-
Reset Out	13
	-
Data Ready –	20
	-
E3	22
E2	23
E1	24
E0	25
P11	26
P10	27
P9	28
P8	29
P7	30
P6	31
P5	32
P4	33
P3	34
P2	35
P1	36
P0	37

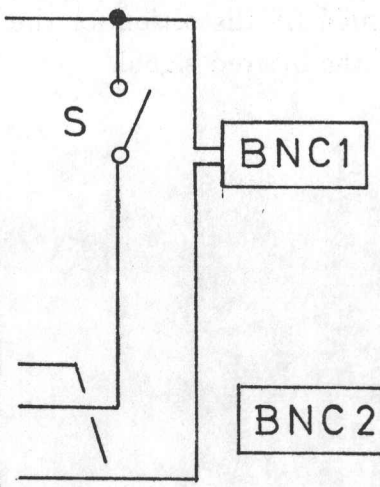

14-Pin male connectors.

Pin	PIA Cassette
2	N4
3	N3
4	N2
5	Ground
6	-
7	N7
8	N1
9	N0
10	N6
11	N5
12	CB2
13	Ground

	PIA-B
2	E0
3	P11
4	P10
5	Ground
6	-
7	E3
8	P9
9	P8
10	E2
11	E1
12	-
13	Ground

	PIA-A
2	P4
3	P3
4	P2
5	Ground
6	CA1
7	P7
8	P1
9	P0
10	P6
11	P5
12	CA2
13	Ground

Processor output:
Ground true TTL.
Pin 13 + true TTL.
Pin 11 not TTL (−5 V).

Fig.A1 37-Wire Side-by-Side Cable.

APPENDIX B - WAVEFORM GENERATION WITH THE PM5138

B.1 Principle

User-defined signals can be produced by the Philips PM5138 function generator by means of the "Arbitrary" function. Signals are constructed point by point on a grid of 1024 by 1023 points:
X-axis: 1024 sample addresses (0 to 1023),
Y-axis: 1023 amplitude values (−511 to +511).
The amplitude value is converted into a voltage by the generator on the basis of 10 V = 511 points; the maximum peak-to-peak amplitude is 20 V, with increments of 10/511 = 0.0196 V.

The 1024 addresses of the signal are sampled at a maximum rate of 20.48 10^6 samples per second; the maximum repetition frequency of the signal at the output is thus 20 kHz.

B.2 Doppler signal generation

Synthetic filtered doppler signals are built as a carrier sine wave (doppler frequency) modulated by a gaussian envelope (modulation frequency). The number $NBURST$ of consecutive doppler bursts generated over the 1024 addresses can be taken as 1, 2 or 4. The first burst is generated over respectively 1024, 512, or 256 addresses by the following equation. The remaining bursts, if any, are generated by a mere replication of amplitude values over the remaining addresses.

Signal amplitude. The maximum amplitude value Y_0 is calculated from the required output peak-to-peak amplitude $AMPL$. The best accuracy in defining the shape of the signal is obtained by programming it with the full 1023-value Y-axis span, i.e by taking $AMPL$=20. The signal amplitude is then adjusted manually after transmission, the generator being in the local mode.

Carrier wave. The frequency of the sine carrier is the doppler frequency. The number of periods NC over one burst is equal to the modulation ratio (§3.1.1). The phase is such that the wave is taken equal to 1 at the middle of the burst X_0, where the maximum of the modulation wave is also found.

Modulation wave. The modulation wave is a gaussian centered on the middle of the burst. The value of B is obtained by requiring the gaussian to fall below a given value Y_2/Y_0 within a distance $DELTAX$. The value chosen for Y_2 is 0.5; $DELTAX$ is calculated by taking into account the burst presence ratio (§3.1.1) $BPRES/100$.

The equation of the waveform is then :

$$Y = Y_0 * \cos\left(\pi * NC * \frac{X - X_0}{X_0}\right) * \exp\left(-(\frac{X - X_0}{B})^2\right)$$

where :

$$Y_0 = \frac{511}{10} * AMPL$$

$$X_0 = \frac{512}{NBURST}$$

$$B = \frac{DELTAX}{\sqrt{\ell n Y_0 / Y_2}}$$

$$DELTAX = \frac{BPRES}{100} * X_0$$

The maximum available doppler and modulation frequencies are determined by the sampling characteristics of the PM5138. It is necessary to digitize every doppler cycle into a minimum number of samples, so as to get a signal shape of good quality. A minimum value of four samples is imposed, though this value is anyway insufficient to let the cycle-counting function of the LDV processor operate correctly (§3.3). The maximum doppler frequency that can be programmed is thus 20.48 $10^6/4 \approx$ 5 MHz. The maximum modulation frequency is respectively 20, 40 or 80 kHz for $NBURST$=1, 2 or 4. A further increase of the modulation frequency should be possible by increasing $NBURST$, but at the expense of either the number of samples per doppler cycle, or the number of cycles in a burst. In the first case signal quality is impaired, in the other case unrealistic doppler signals are generated.

When the number of samples per doppler cycle is large enough, it is not necessary to define the signal by a full set of 1024 addresses, which leads to very cumbersome transmissions. It is possible to program interactively the digitization into a smaller number of samples K ($K = 2^x$, $4 \leq x \leq 10$), as long as a minimum number of four cycles is kept in a doppler burst.

B.3 GPIB implementation

Programming the generator is made by a PC-AT via a GPIB/IEEE 488 interface. A Tektronix GPIB-PC2A (National Instruments) card installed on the PC is implemented with the TEK GURU driver software. Commands are sent as character strings ($\leq$ 255 characters), including the sequence of amplitude values required to define the signal, because the generator does not accept binary files. The capacity of a command string is about 48 five-character (incl. separator) values; up to 24 consecutive strings may be necessary to program one signal.

The implementation of the TEK GURU software with the PM5138 has not been very successful. Two kinds of problems were occasionally met during the transmissions :

- PC crashes with or without "Parity check" warning messages,

- failure of the PM5138, in the "Arbitrary" mode, to set the desired frequency or voltage amplitude, or to catch the waveform.

Examination of the GPIB status byte, after every completed transmission, did not indicate any GPIB error. On the contrary, the presence of PM5138 errors was revealed by the examination of the error string of the generator. According to the manufacturer of the PM5138, this problem is related to a lack of complete compatibility between the TEK GURU driver and the generator, concerning particularly the transmission rates. Note that changing the timeout values in the GPIB transmission did not solve the problem. The solution proposed by the manufacturer is to use the Philips driver* software.

Due to the occasional character of the transmission problem, it was nevertheless succeeded in programming appropriate signals by taking the following precautions :

- Before the transmission, generator in local mode, as many settings as possible are preset manually, according to the values programmed in the command strings. This involves mainly the repetition frequency and the amplitude of the signal. Failure opportunities are avoided by preventing the generator from switching them internally.

- As long as signal modifications involve only repetition frequency and signal amplitude, and not the shape of the signal, the modifications are made manually in the local mode, avoiding to perform new transmissions.

* GPIB Drivers Software for National Instruments card PC-2A/2B : Philips PM2201/52.

APPENDIX C - THE DATA ACQUISITION SYSTEM (DAS)

The acquisition (Fig. 4) is performed with a commodore CBM 8032 microcomputer and a Commodore extension interface (CEI). The DAS is designed to perform LDV measurements with the TSI processor; the main functions are

- to ensure a fast transfer of data into microcomputer memory,
- to transfer data on cassette tape for further processing on the VAX cluster.

The procedure is adapted from that used in the von Karman S-1 wind tunnel by the AR department. Modifications are introduced in order to meet specific requirements :

- switching from NC to SMB mode,
- improving the acquisition rate,
- measuring the acquisition rate,
- measuring the percentage of data actually processed (acceptation percentage),
- skipping data, in order to keep only every n^{th} sample.

Modifications are implemented either in the hardware (new 37-wire cable) or in the software (modified assembler and new Basic programs).

C.1 Principle of operation

Data are available at the output 37-pin connector in of the processor in the following format:

Number of cycles: 8 bits N0-N7
Period exponent: 4 bits E0-E3
Period mantissa: 12 bits P0-P11

Data are led via a 37-wire cable (Fig. A1) to the data registers of two Motorola MC 6820 PIA's in the CEI.

1. PIA-A Register A: P0-P7
   PIA-B Register B: LSB P8-P11; MSB E0-E3
2. PIA Cassette Register A: used to transfer data to TEAC tape
   Register B: N0-N7

Data transfer is under control of the TSIACQ.OBJ assembler program which is accessed from the Basic TSIACQ program. The data ready pulse from the processor is detected on the CA1 peripheral input line of PIA-A. An inhibition signal delivered by the CA2 peripheral control line of PIA-A prevents updating the output register of the processor. PIA registers are read sequentially, their contents is stored into 3 bytes of mi-

crocomputer memory and the inhibition is cleared. Up to sixty pages of 256 bytes allow for 85 to 5100 data sets to be stored. Control is given back to the Basic program once the requested number of pages is filled. Data transfer to cassette tape is performed via the TEAC assembler routines located in CEI EPROM.

C.2 Switching from NC to SMB mode

A manual switch S is mounted on the cover of the 37-pin male connector on the cable; closing the switch grounds pin 11 (Fig. A1) and selects the SMB mode (§2.2.3). Note that pin 11 is not TTL compatible. The measured level is −5 V with respect to the ground (low TTL). It was therefore not possible to command mode switching by the computer, e.g. via the CB2 control line of PIA-B.

C.3 Improving the acquisition rate

The acquisition rate is fixed by the number of machine cycles required to execute one loop of the assembler program. One machine cycle is 1 μs long (1 MHz 6502 microprocessor).

The TSI10D85B4 assembler program written by F. Thiry for the S1 features a 160 machine cycles acquisition loop, i.e., a 6 kHz acquisition rate; data are stored in a 3-kbyte buffer (1024 data sets); the program includes an automatic transfer of data on tape when the buffer is full; measurements completed by the processor during this transfer are lost.

In order to increase the acquisition rate this program was thoroughly modified :

- Data acquisition and data transfer to tape are separated, with distinct entry points in the assembler program.
- Filling up to 15 kbytes of memory is made possible.
- The length of the acquisition loop is drastically reduced by avoiding calls to subroutines, and by suppressing the check for loss of data during an acquisition loop.

The resulting TSIACQ.SRC program features a 61 cycles acquisition loop, i.e., a 16 kHz acquisition rate.

C.4 Measuring the acquisition rate

In order to measure the acquisition rate, the time necessary to put a large number of data into memory is measured with a Philips PM 6671 timer/counter in the PULSE WIDTH mode. The assembler program delivers a pulse via the CB2 control line of the PIA-Cassette; the pulse is fed to the timer via the female BNC2 connector on the 37-wire cable (Fig. A1). The pulse starts at the first data ready check and ends with the return to the Basic.

The shortest measured acquisition time is 66 μs, corresponding to 15.2 kHz. This result is obtained in the NC mode (type A signals, N_m=8) at doppler frequencies of 5 MHz and up, and in the SMB mode (type B, N_m=8, MR=20 or 100) at 20 MHz. There is a very good agreement with the predicted value.

C.5 The acceptation percentage - Practical acquisition rate

By comparing the number of data recorded, with the number of system resets of the TSI processor, it is possible to evaluate the capacity of the DAS to avoid missing data. The number of resets being roughly equal to the number of measurements initiated by the processor, the difference corresponds :
1) to aborted measurements,
2) to measurements performed during inhibition, which do not update the output register of the processor.

The acceptation percentage is defined as 100 times the ratio of recorded measurements to system resets. When synthetic signals are used, aborted measurements are unlikely; the acceptation percentage measures actually the efficiency of the DAS. It allows to estimate the number of measurements lost during the dead time corresponding to the inhibition.

The number of resets is counted on the Philips PM 6671 timer/counter in the COUNT GATED BY B mode; the reset pulses issued by the processor are fed to the A input of the counter, via the female BNC1 connector on the 37-wire cable (Fig. A1); the gating pulse at input B is the same as that used to measure the acquisition rate (§C.4). Measurements of the acceptation percentage yield high values (> 90%) for acquisition rates up to 10 kHz, either in the NC mode (type A signals, N_m=8) where the acquisition rate is determined by the time the processor requires to process the Doppler signal, or in the SMB mode (type B, N_m=8, MR=20 or 100), where it is fixed by the burst rate. At higher values of the aquisition rate, the acquisition time of the DAS becomes gradually the limiting factor, and the acceptation percentage decreases quickly.

It can be concluded that, though the DAS is able to store data at a maximum rate of about 15 kHz, the practical limit in LDV measurements, set by the necessity of preserving particle statistics, and thus of avoiding missing data, is 10 kHz.

C.6 Skipping data

In order to estimate correctly time averages it is necessary to record data over a time lapse much larger than the characteristic period of the flow. Owing to the rather low capacity of data storage (5100), it may be difficult to get a data rate low enough to satisfy this requirement. The possibility of recording only a part of the data present at the output of the processor without altering data statistics is therefore interesting. For that purpose, the possibility of skipping data, by reading only every $n^{th}(2 \leq n \leq 255)$ is

provided by inserting a loop in the assembler, after the data ready detection. The length of the acquisition loop becomes 73 μs, plus 21 μs per data skipped; the acquisition rate is correspondingly reduced.

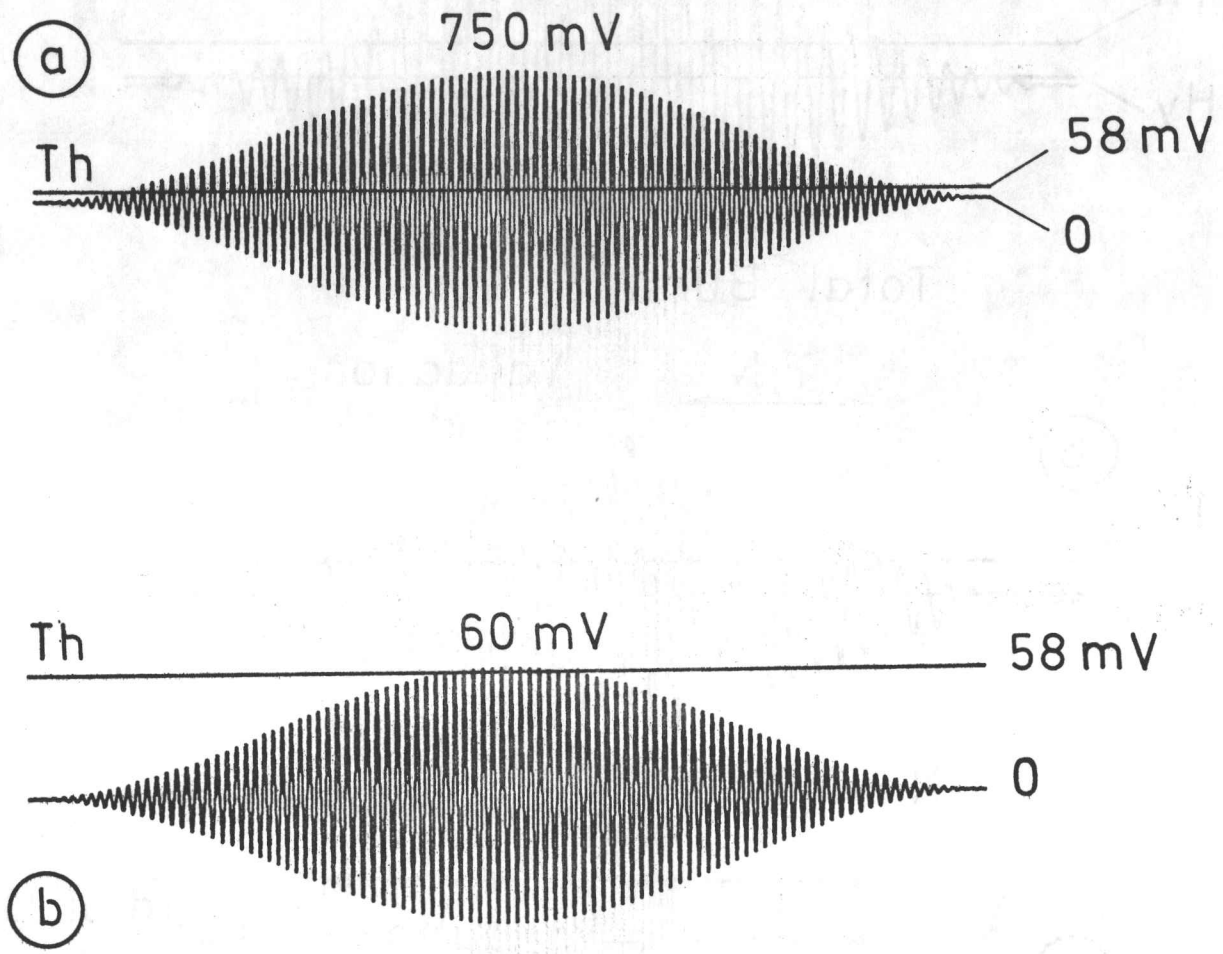

FIG. 1 - INFLUENCE OF SIGNAL STRENGTH ON CYCLE-COUNTING

Th : Threshold 58 mV

a) Strong signal (750 mV) - 80 cycles detected

b) Weak signal (60 mV) - 8 cycles detected

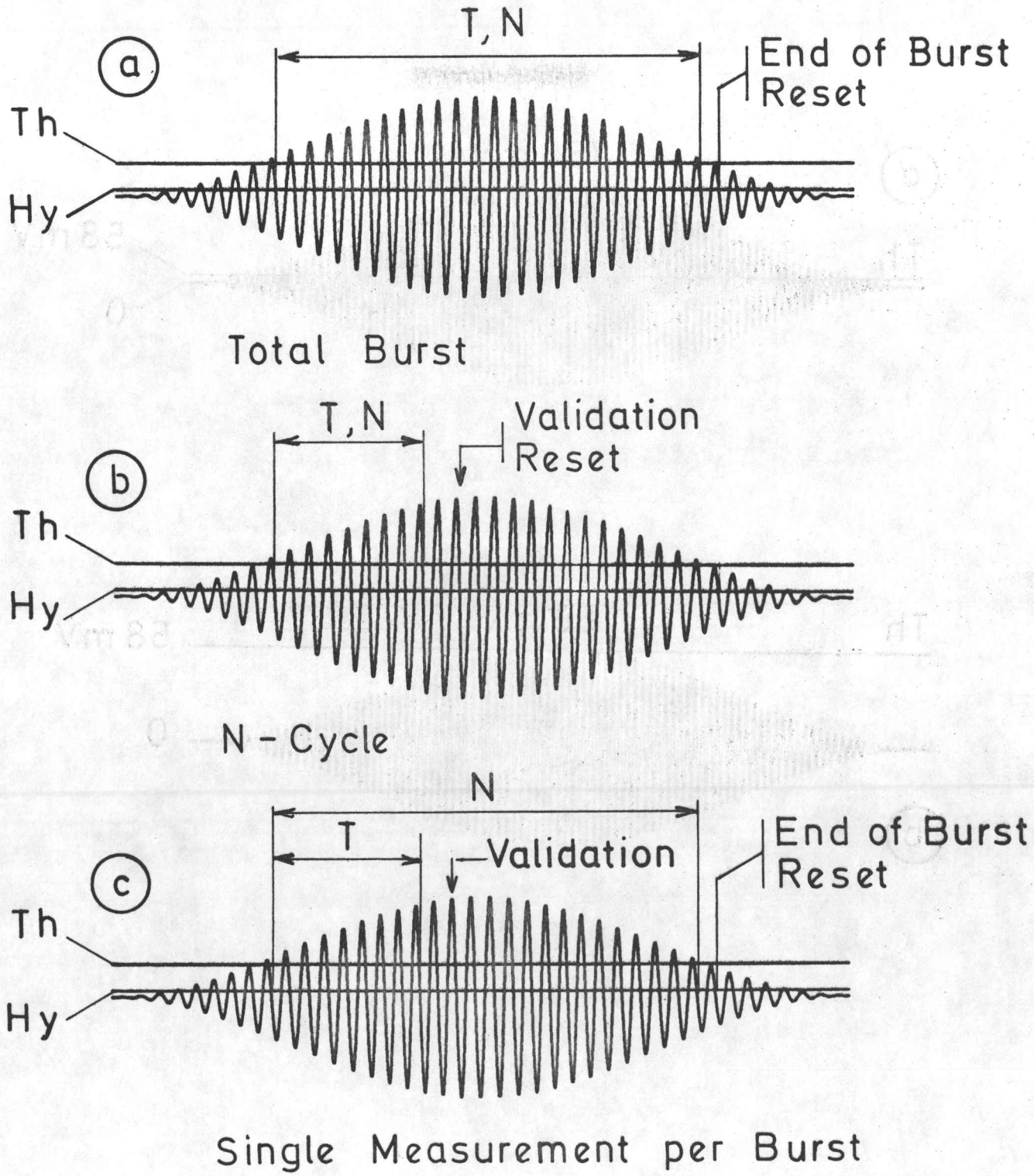

FIG. 2 - THE OPERATING MODES OF THE TSI 1980/1990 PROCESSOR

N : number of cycles delivered at output
T : time delivered at output
Th : threshold level - 50 mV
Hy : hysteresis level - 10 mV

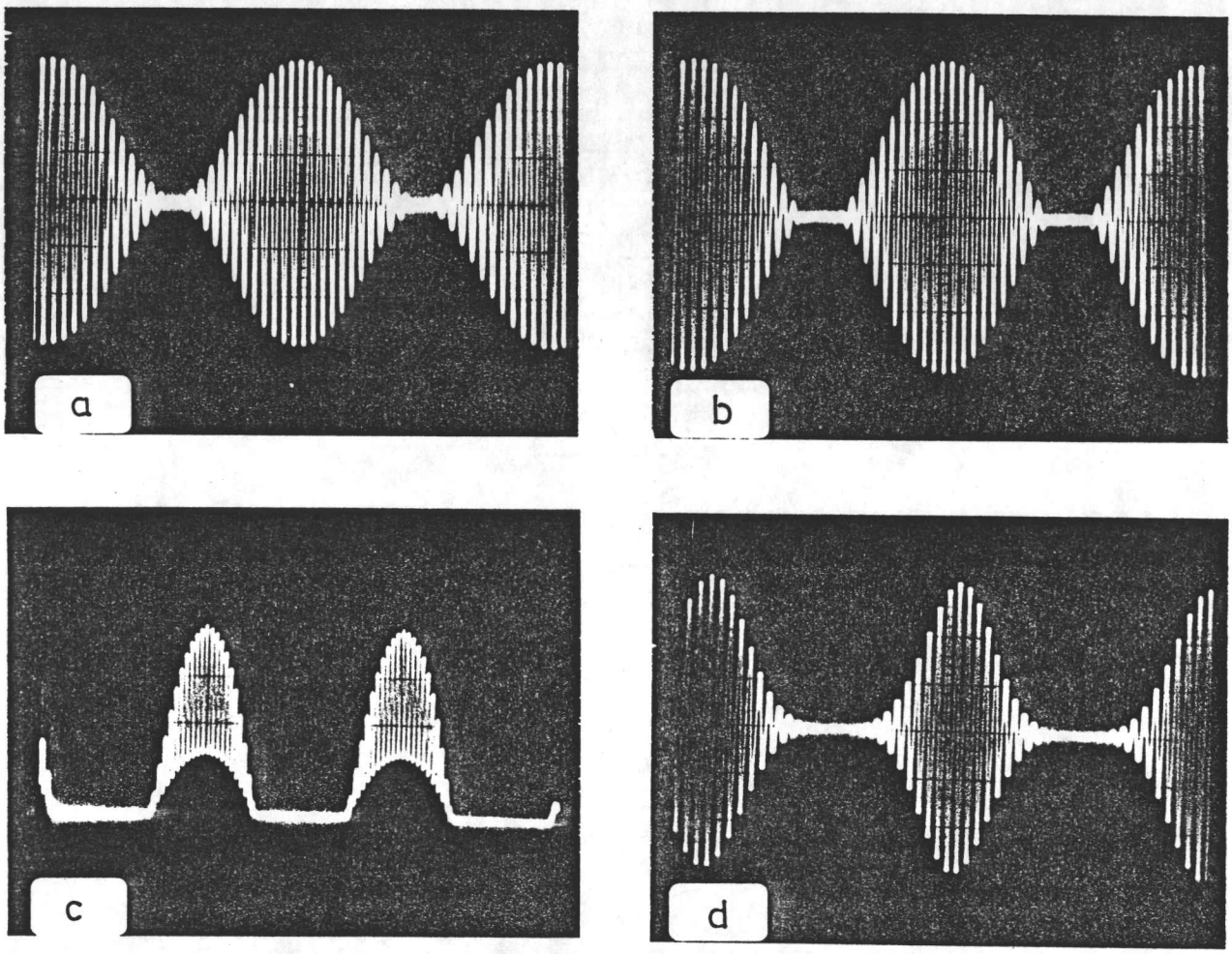

FIG. 3 - SYNTHETIC DOPPLER SIGNALS

a) Type B; MR = 25, BPR = 100%
b) Type B; MR = 25, BPR = 80%
c) Type C; MR = 40, BPR = 50%
d) Type D; MR = 25, BPR = 100%; bandpass filtered ($\nu_D/10$ to $3\nu_D$)

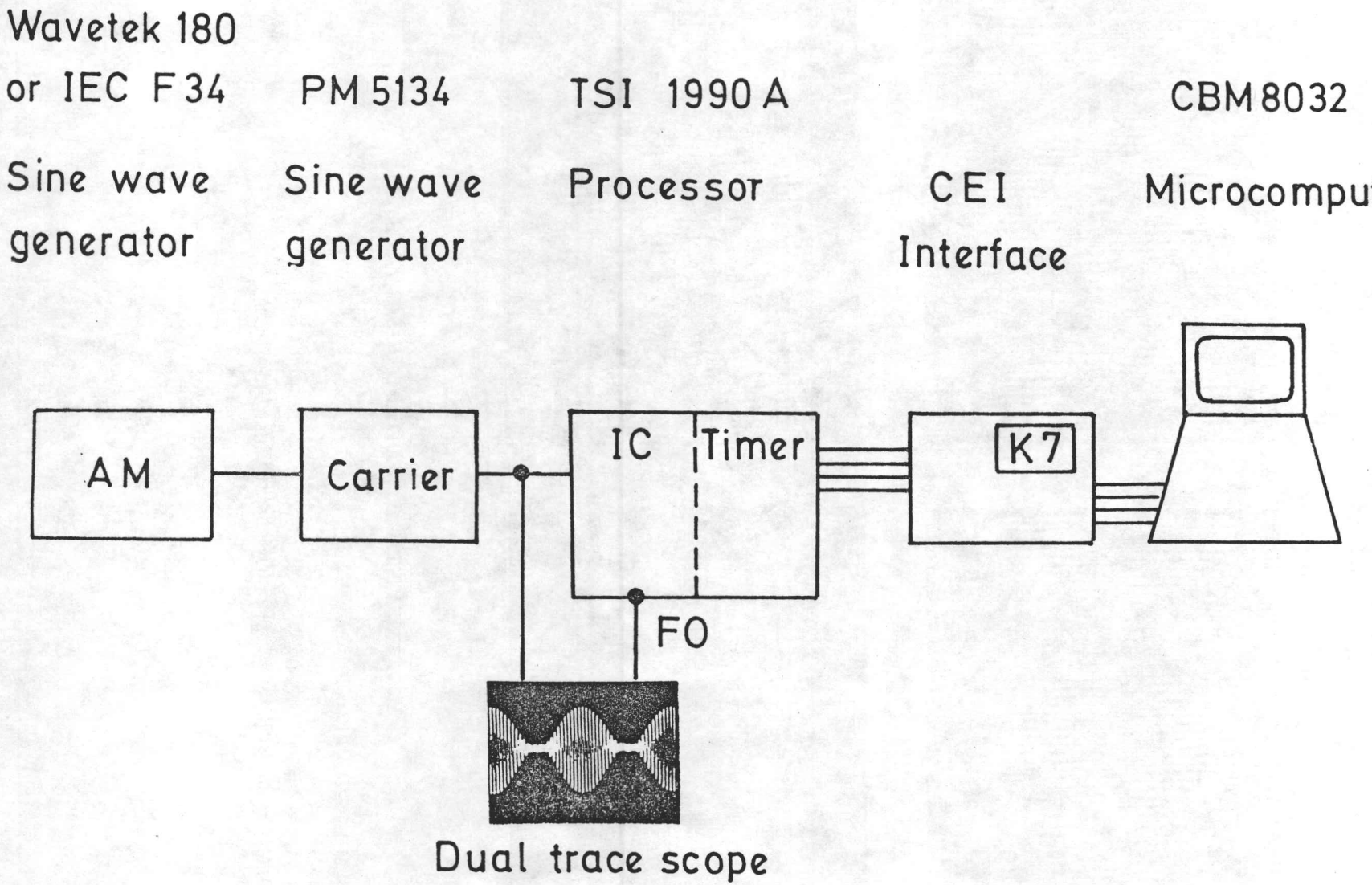

FIG. 4 - DATA ACQUISITION SYSTEM FOR TYPE B SIGNALS

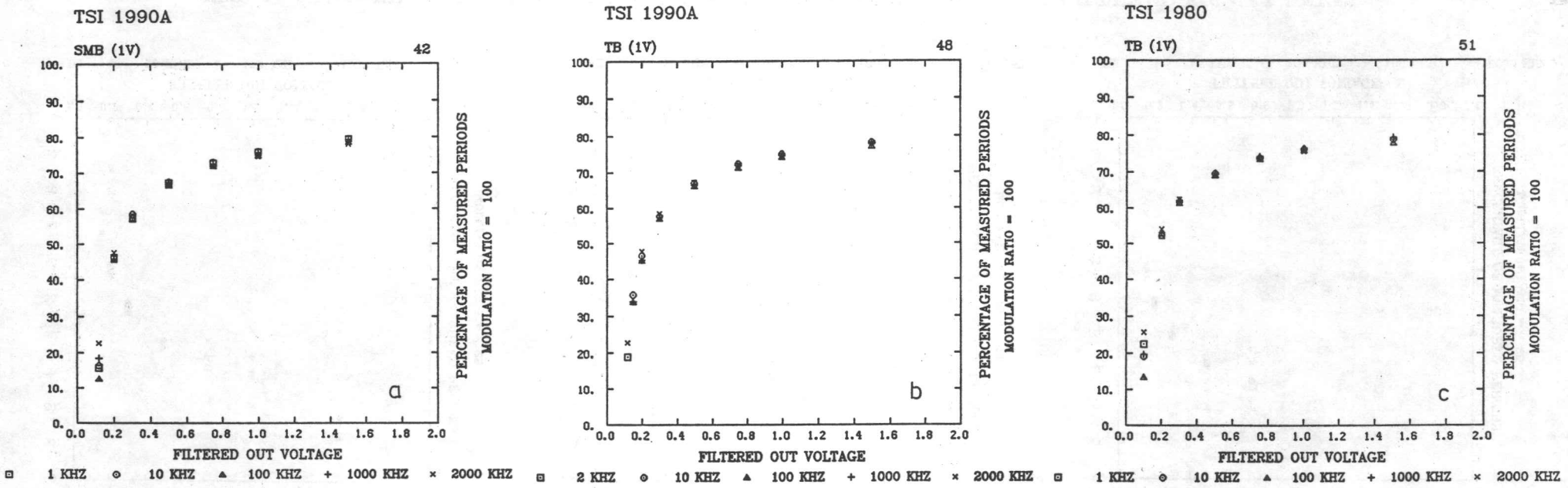

FIG. 5 - NUMBER OF DOPPLER CYCLES MEASURED (PERCENTAGE) VS FILTERED SIGNAL LEVEL

$N_m = 8$; MR = 100; type B signals; doppler frequency 1 kHz to 2 MHz

a) 1990A, SMB mode; b) 1990A, TB mode; c) 1980, TB mode

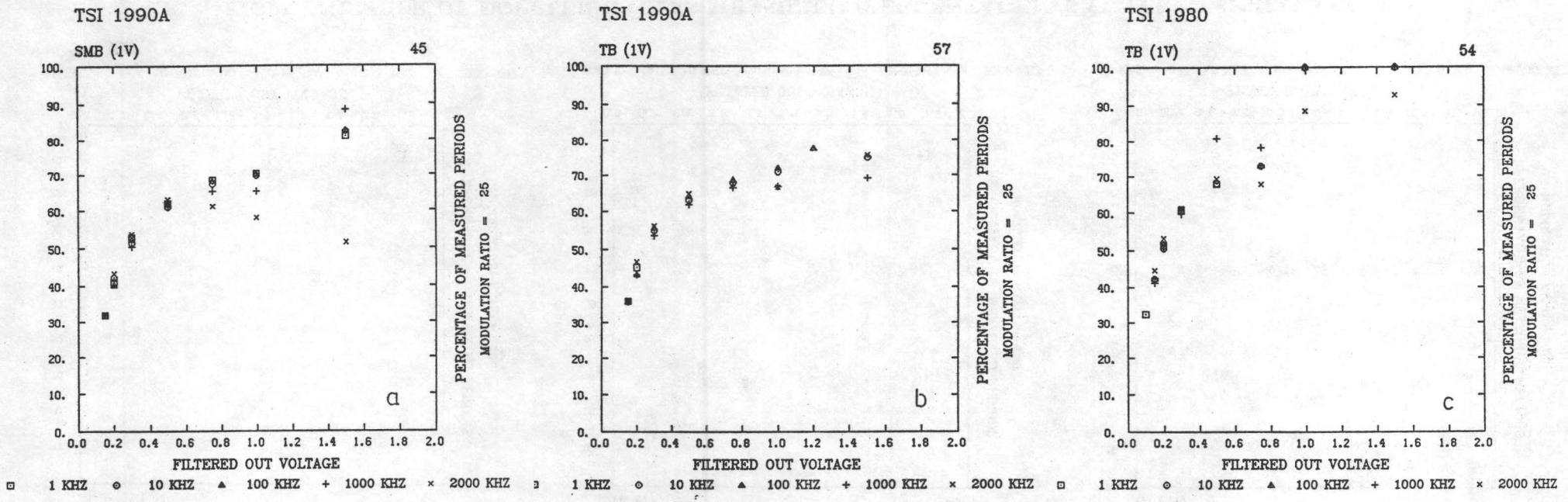

FIG. 6 - NUMBER OF DOPPLER CYCLES MEASURED (PERCENTAGE) VS FILTERED SIGNAL LEVEL

N_m = 8; MR = 25; type B signals; doppler frequency 1 kHz to 2 MHz

a) 1990A, SMB mode; b) 1990A, TB mode; c) 1980, TB mode

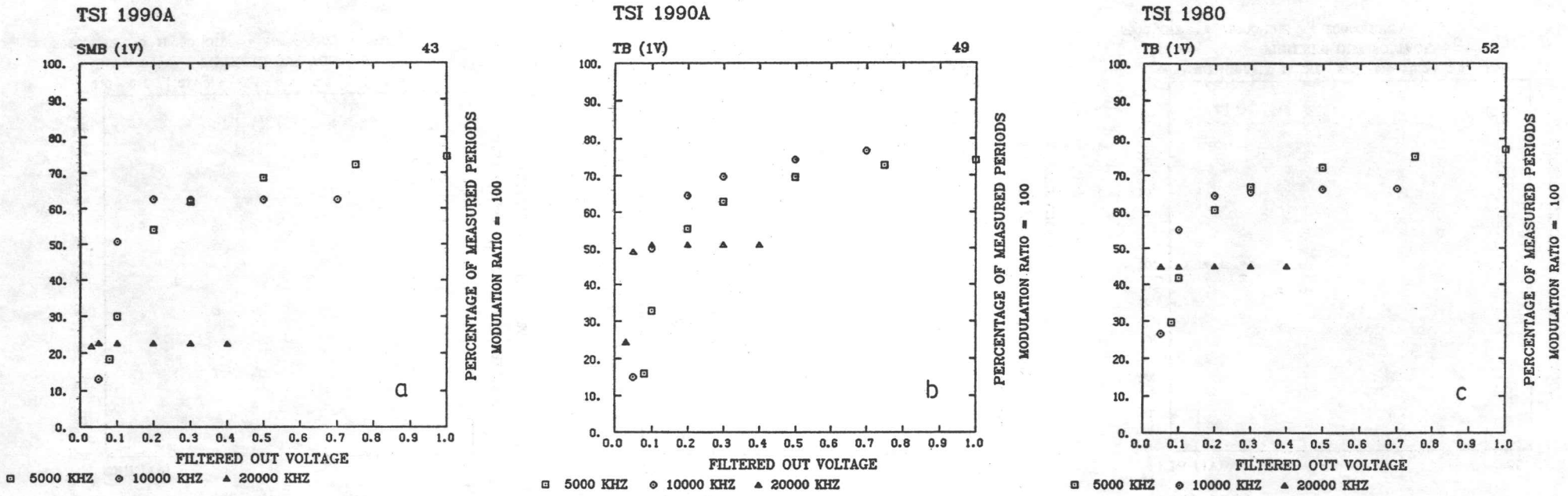

FIG. 7 - NUMBER OF DOPPLER CYCLES MEASURED (PERCENTAGE) VS FILTERED SIGNAL LEVEL

$N_m = 8$; MR = 100; type B signals; doppler frequency 5, 10, and 20 MHz

a) 1990A, SMB mode; b) 1990A, TB mode; c) 1980, TB mode

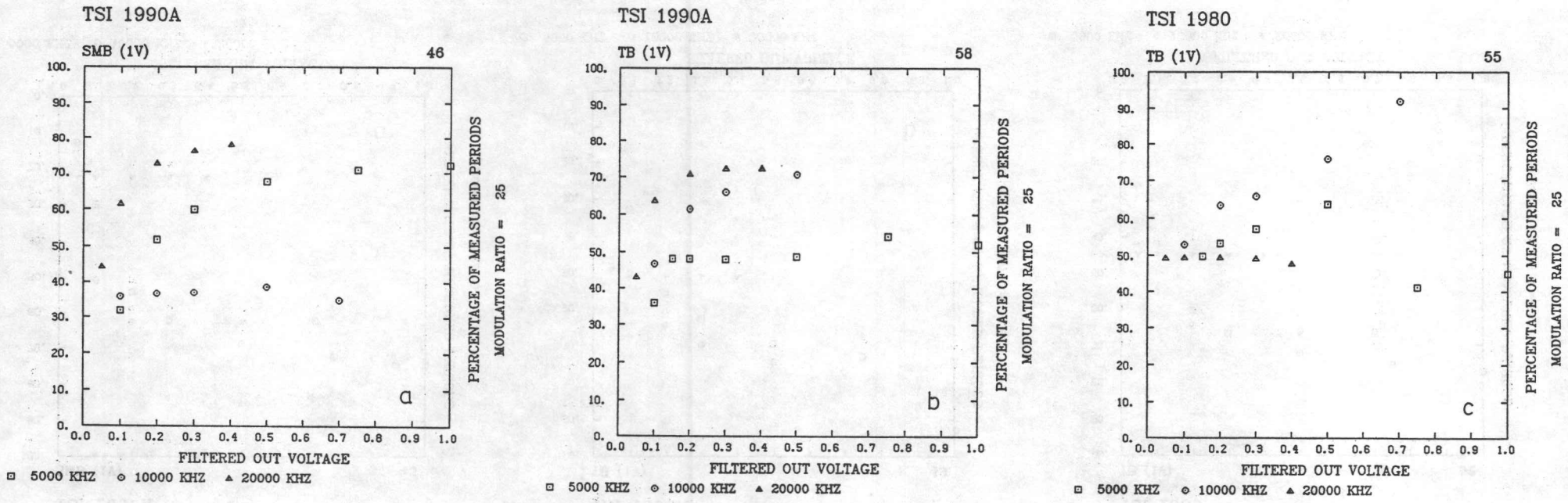

FIG. 8 - NUMBER OF DOPPLER CYCLES MEASURED (PERCENTAGE) VS FILTERED SIGNAL LEVEL

$N_m = 8$; MR = 25; type B signals; doppler frequency 5, 10, and 20 MHz

a) 1990A, SMB mode; b) 1990A, TB mode; c) 1980, TB mode

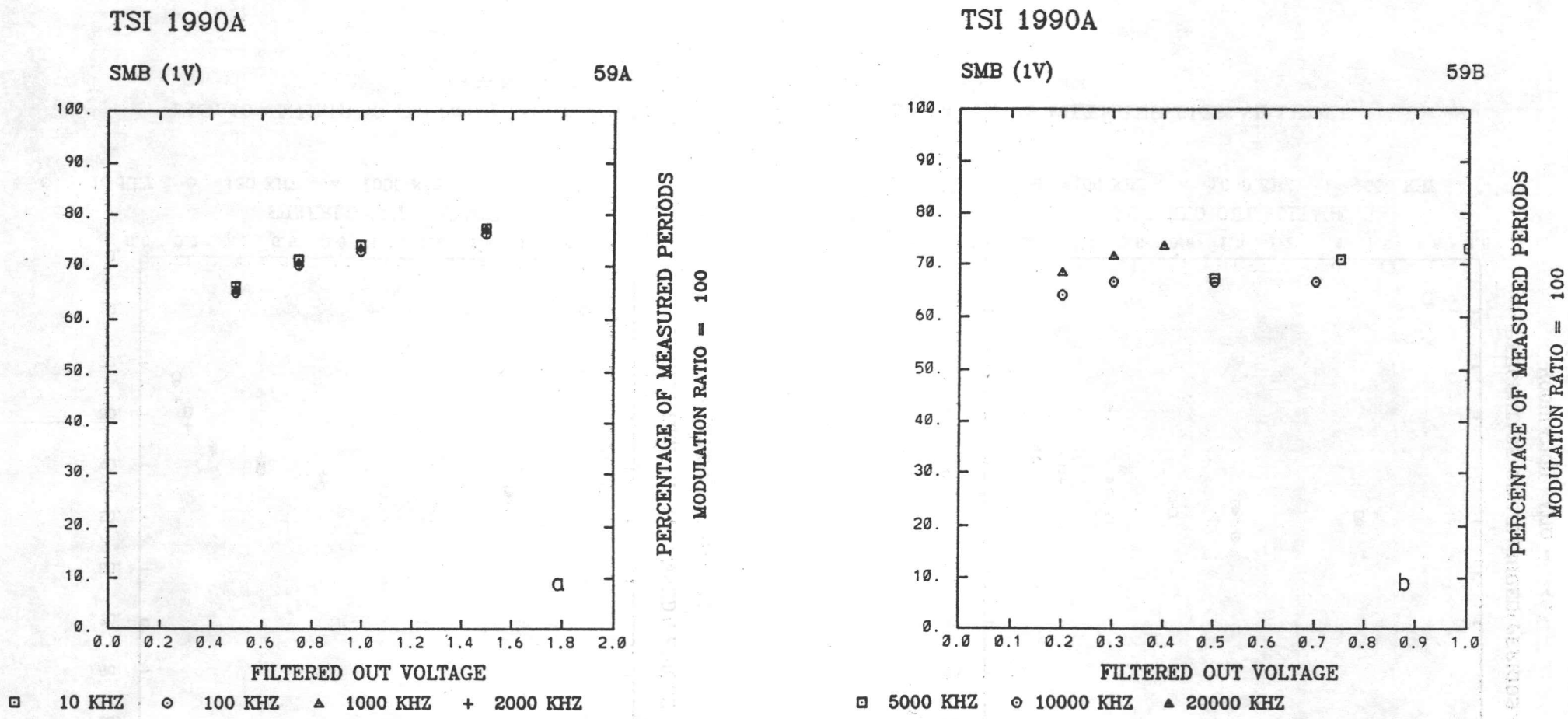

FIG. 9 - NUMBER OF DOPPLER CYCLES MEASURED (PERCENTAGE) VS FILTERED SIGNAL LEVEL

N_m = 64; MR = 100; type B signals; 1990A, SMB mode

a) Doppler frequency 10 kHz to 2 MHz b) 5, 10, and 20 MHz

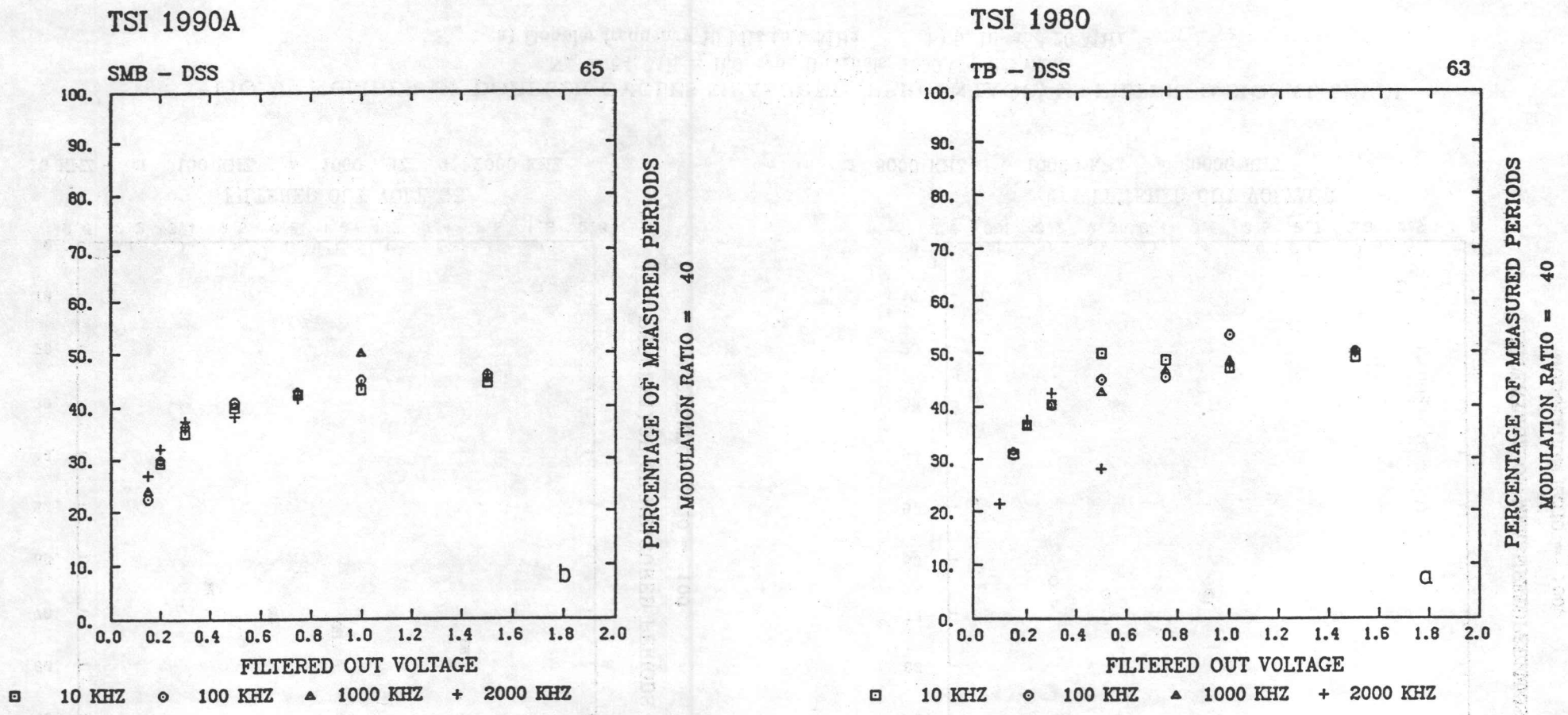

FIG. 10 - NUMBER OF DOPPLER CYCLES MEASURED (PERCENTAGE) VS FILTERED SIGNAL LEVEL

$N_m = 8$; MR = 40; type C signals; doppler frequency 10 kHz to 2 MHz

a) 1990A, SMB mode; b) 1980, TB mode

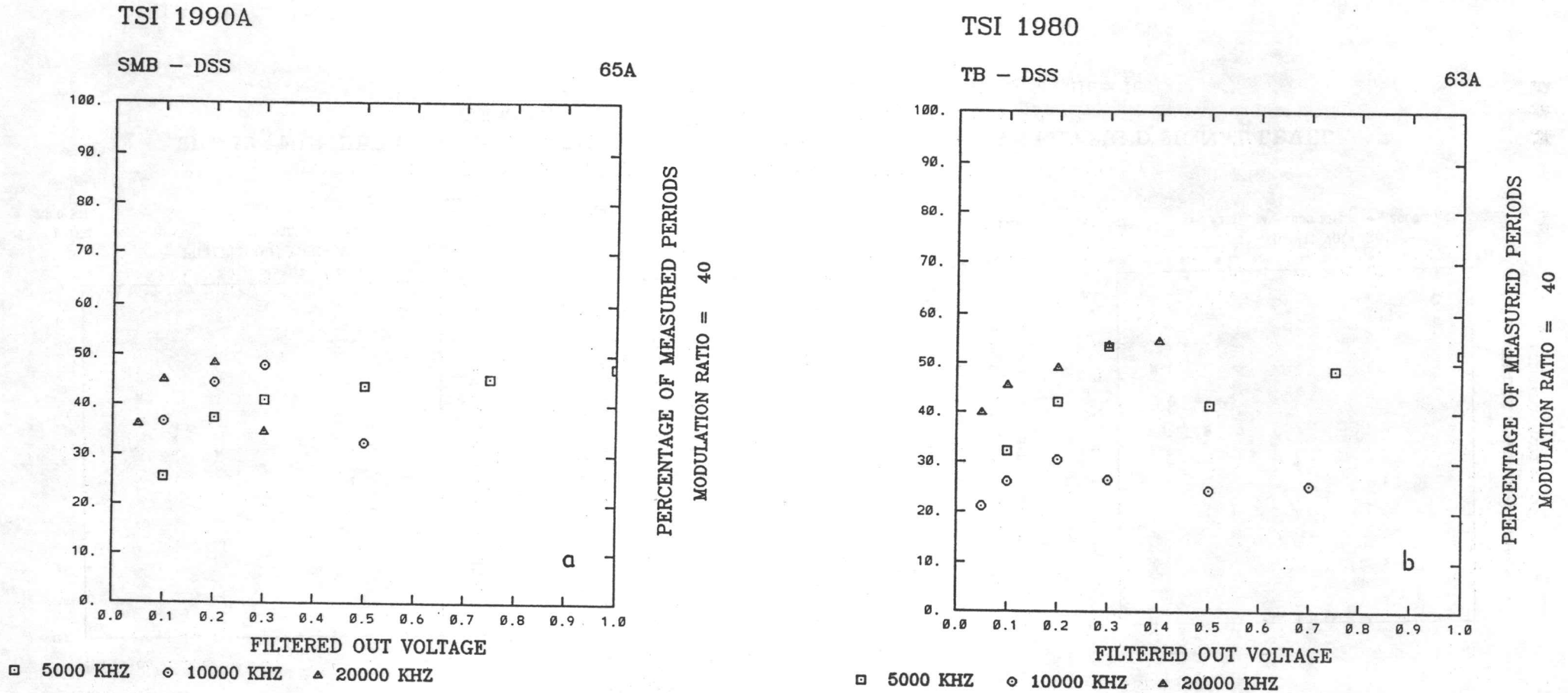

FIG.11 - NUMBER OF DOPPLER CYCLES MEASURED (PERCENTAGE) VS FILTERED SIGNAL LEVEL

$N_m = 8$; MR = 40; type C signals; doppler frequency 5, 10, and 20 MHz

a) 1990A, SMB mode; b) 1980, TB mode

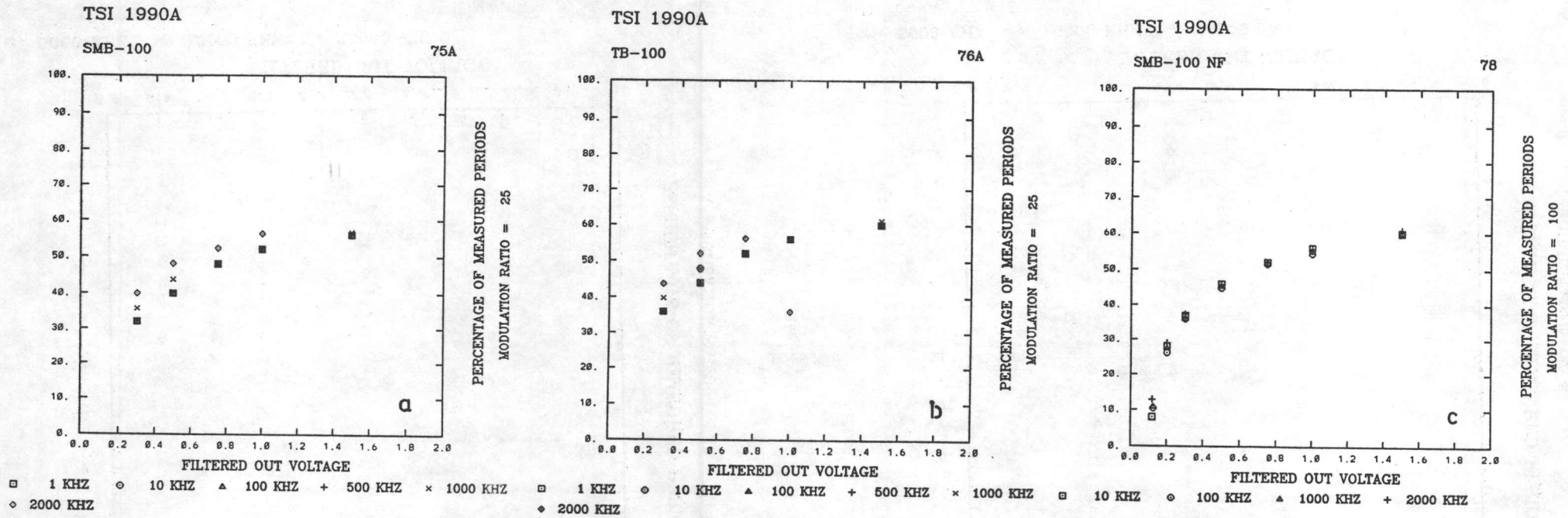

FIG. 12 - NUMBER OF DOPPLER CYCLES MEASURED (PERCENTAGE) VS FILTERED SIGNAL LEVEL

1990A; $N_m = 8$; type D signals; doppler frequency 1 kHz to 2 MHz

a) SMB mode, MR = 25; b) TB mode, MR = 25; c) SMB mode, MR = 100

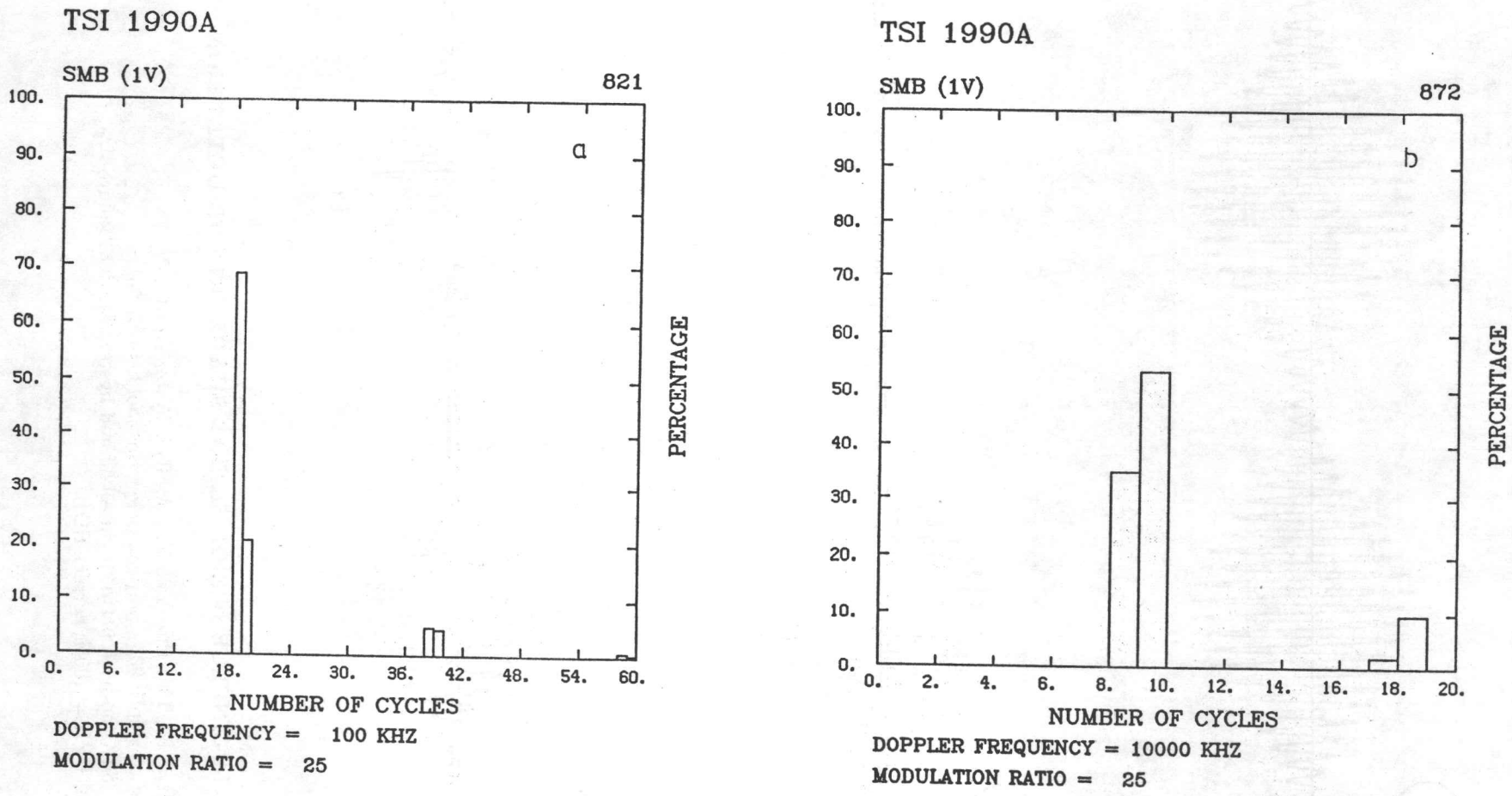

FIG. 13 - HISTOGRAMS OF DOPPLER CYCLE COUNTS

N_m = 8; MR = 25; type B signals; 1990A, SMB mode

a) High-counts at 100 kHz - 1.5 V from Fig. 6a

b) Low-counts at 10 MHz - 0.5 V from Fig. 8a

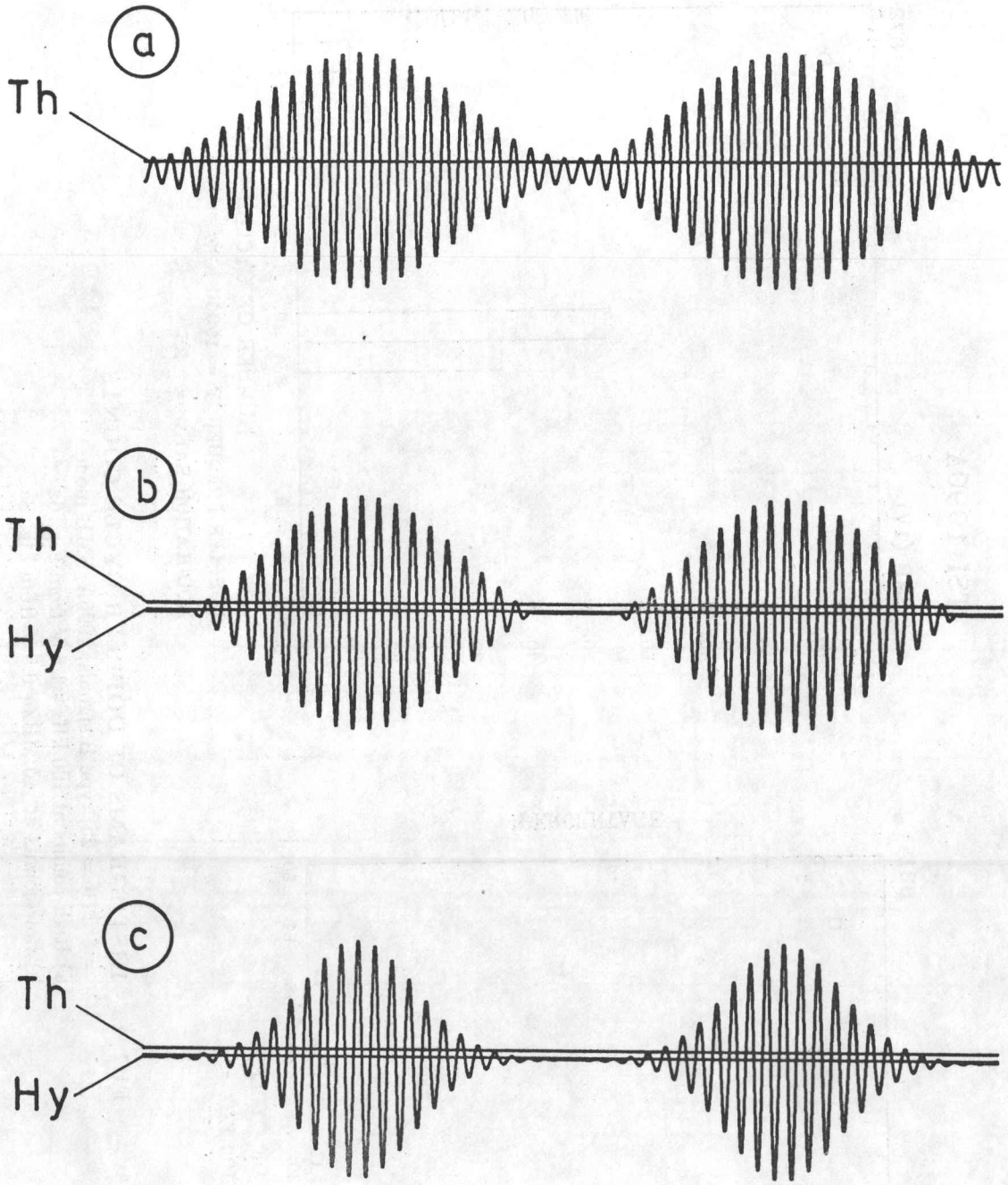

FIG. 14 - INFLUENCE OF SIGNAL SHAPE ON EOB DETECTION

Signal 750 mV, MR = 25; Th : threshold 58 mV, Hy : hysteresis 10 mV
a) Type B, modulation depth 90%; no peak below threshold; EOB failure
b) Type B, BPR = 80%; no peak between threshold and hysteresis; EOB failure
c) Type D gaussian, BPR = 100%; correct EOB

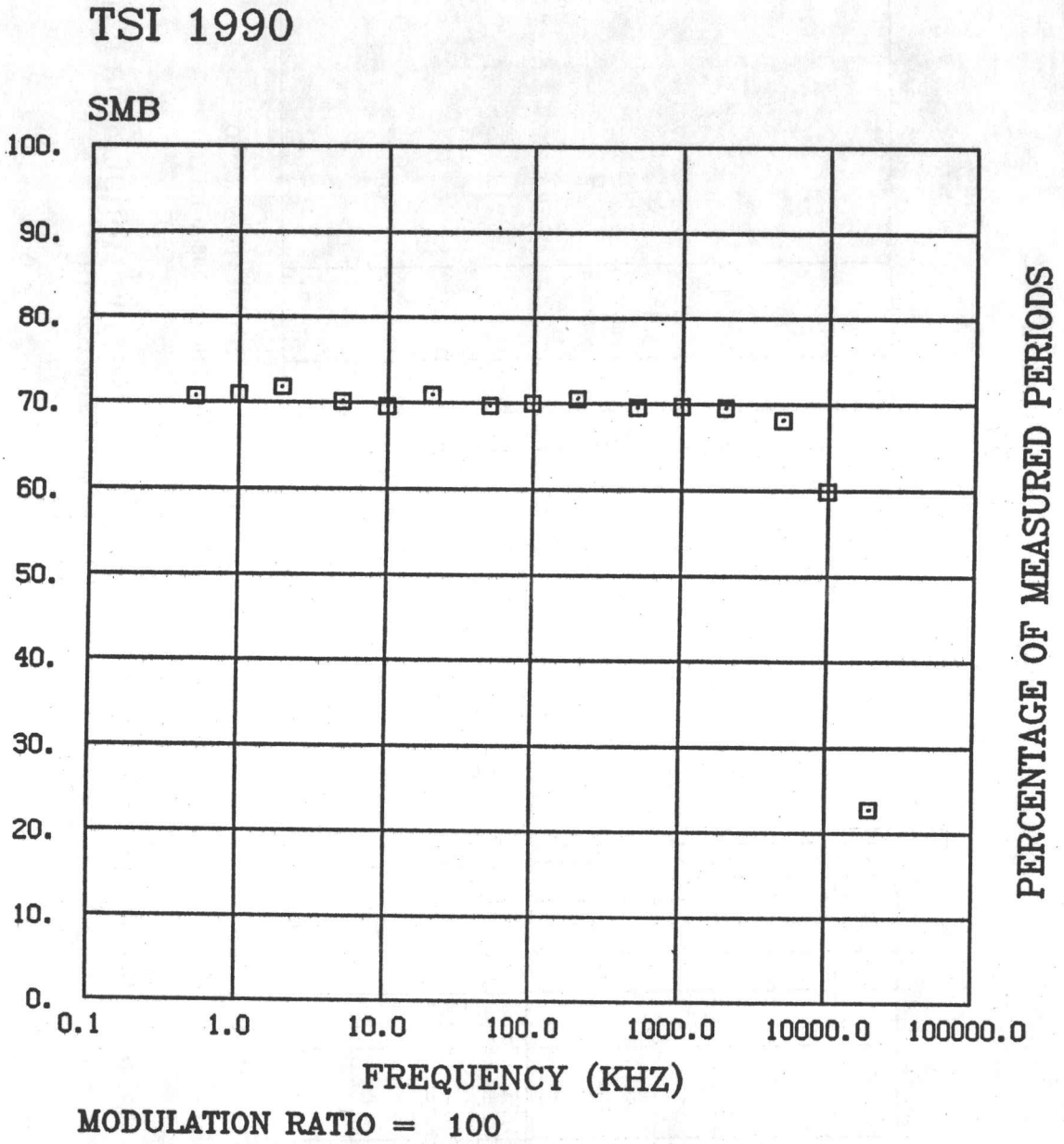

FIG. 15 - NUMBER OF DOPPLER CYCLES MEASURED (PERCENTAGE) VS DOPPLER FREQUENCY

1990A; SMB mode; $N_m = 8$; MR = 100; type B signals

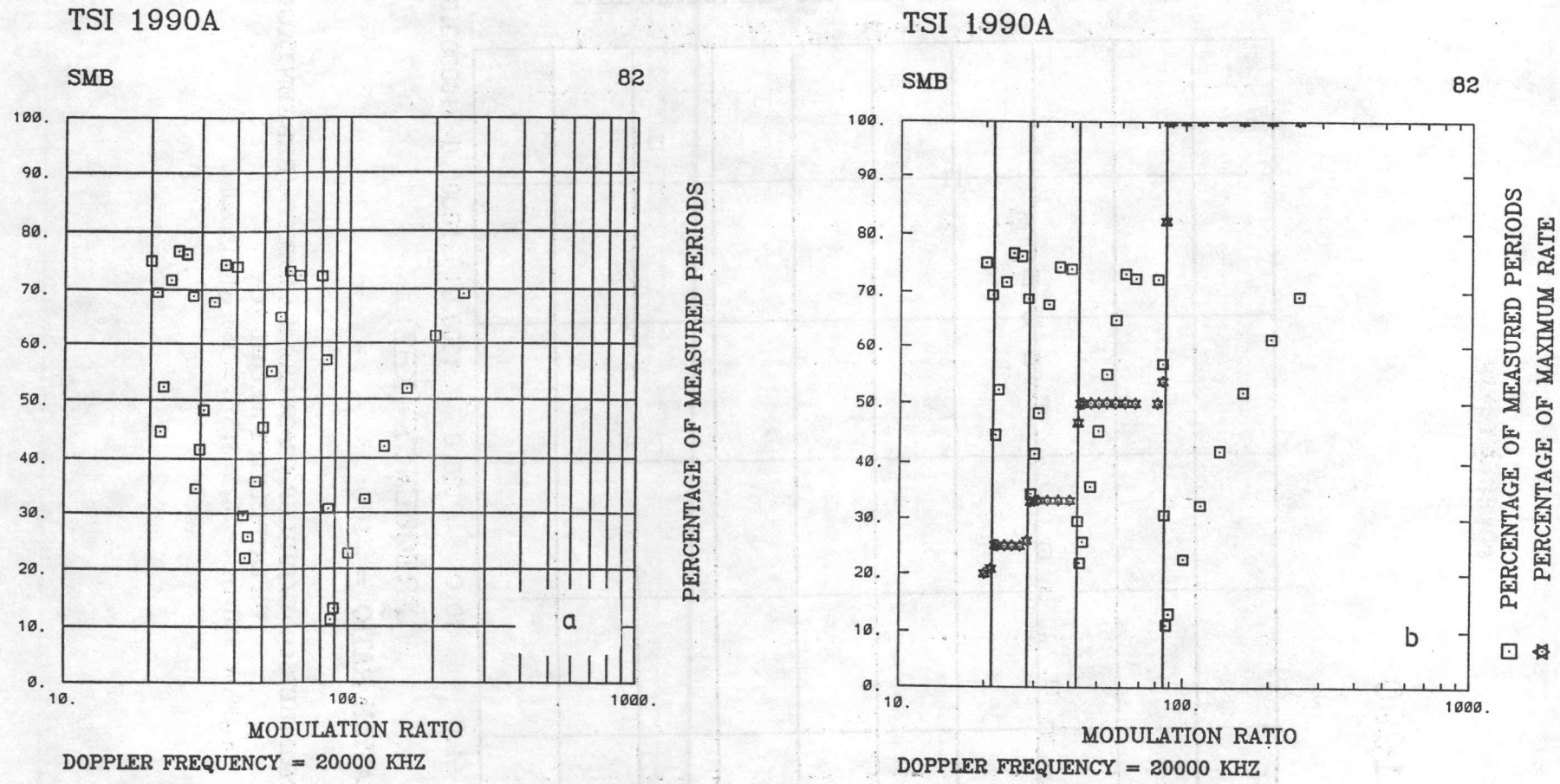

FIG. 16 - NUMBER OF DOPPLER CYCLES MEASURED (PERCENTAGE) VS MODULATION RATIO

1990A; SMB mode; $N_m = 8$; type B signals; doppler frequency 20 MHz

a) Number of cycles b) Number of cycles and data rate

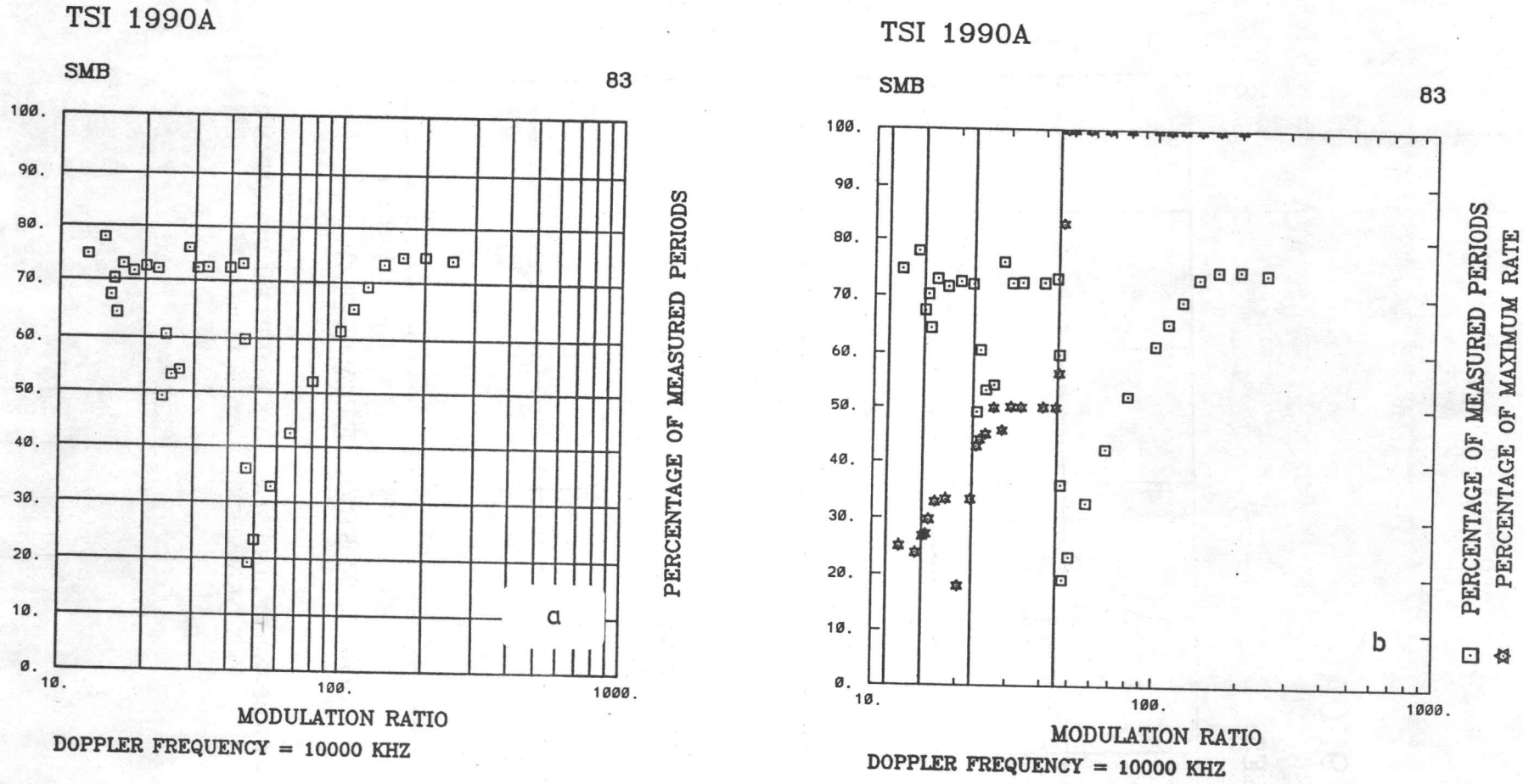

FIG. 17 - NUMBER OF DOPPLER CYCLES MEASURED (PERCENTAGE) VS MODULATION RATIO

1990A; SMB mode; $N_m = 8$; type B signals; doppler frequency 10 MHz

a) Number of cycles b) Number of cycles and data rate

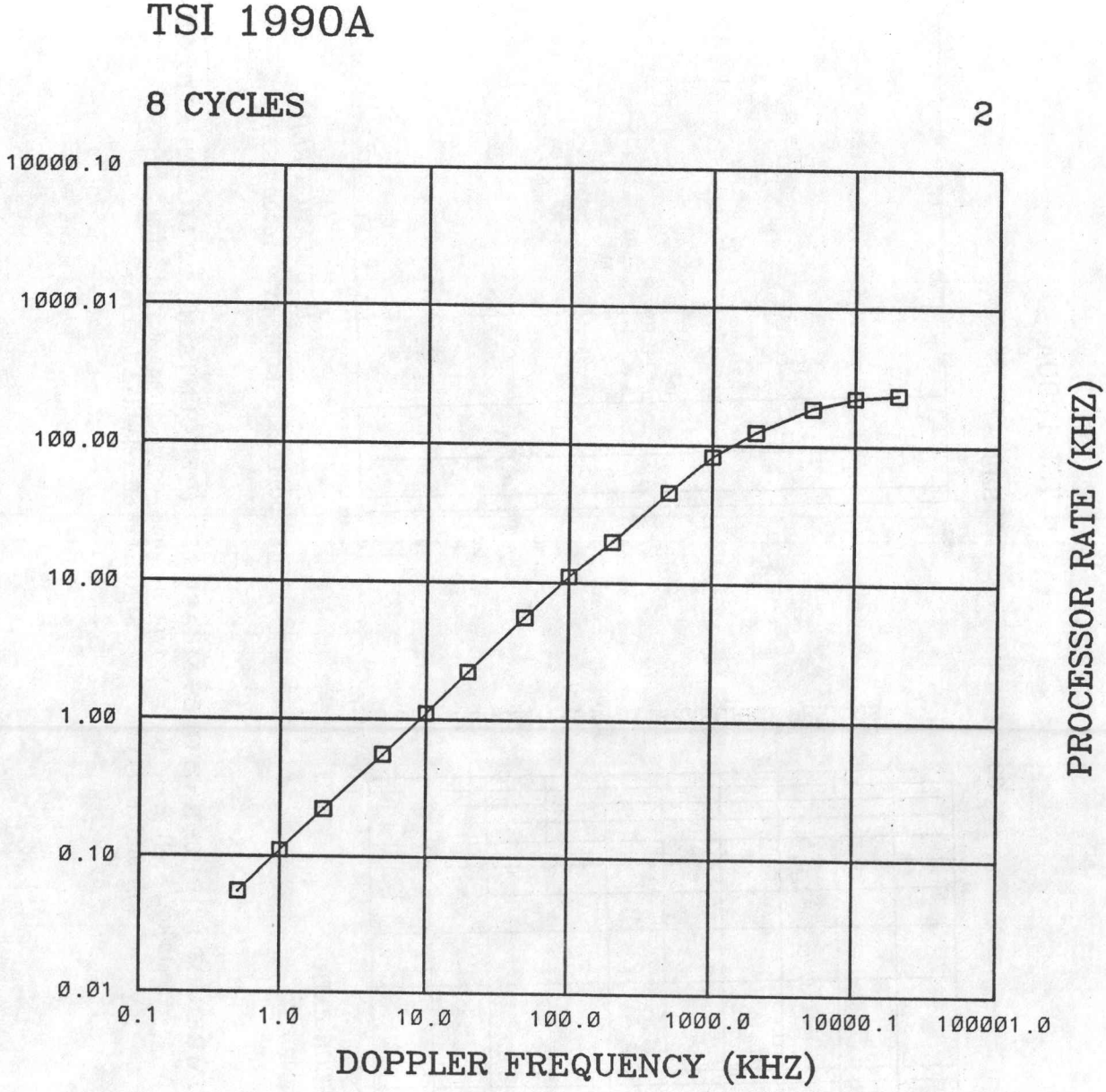

FIG. 18 - FREE-WHEELING RATE VS DOPPLER FREQUENCY
1990A; NC mode; $N_m = 8$; type A signals

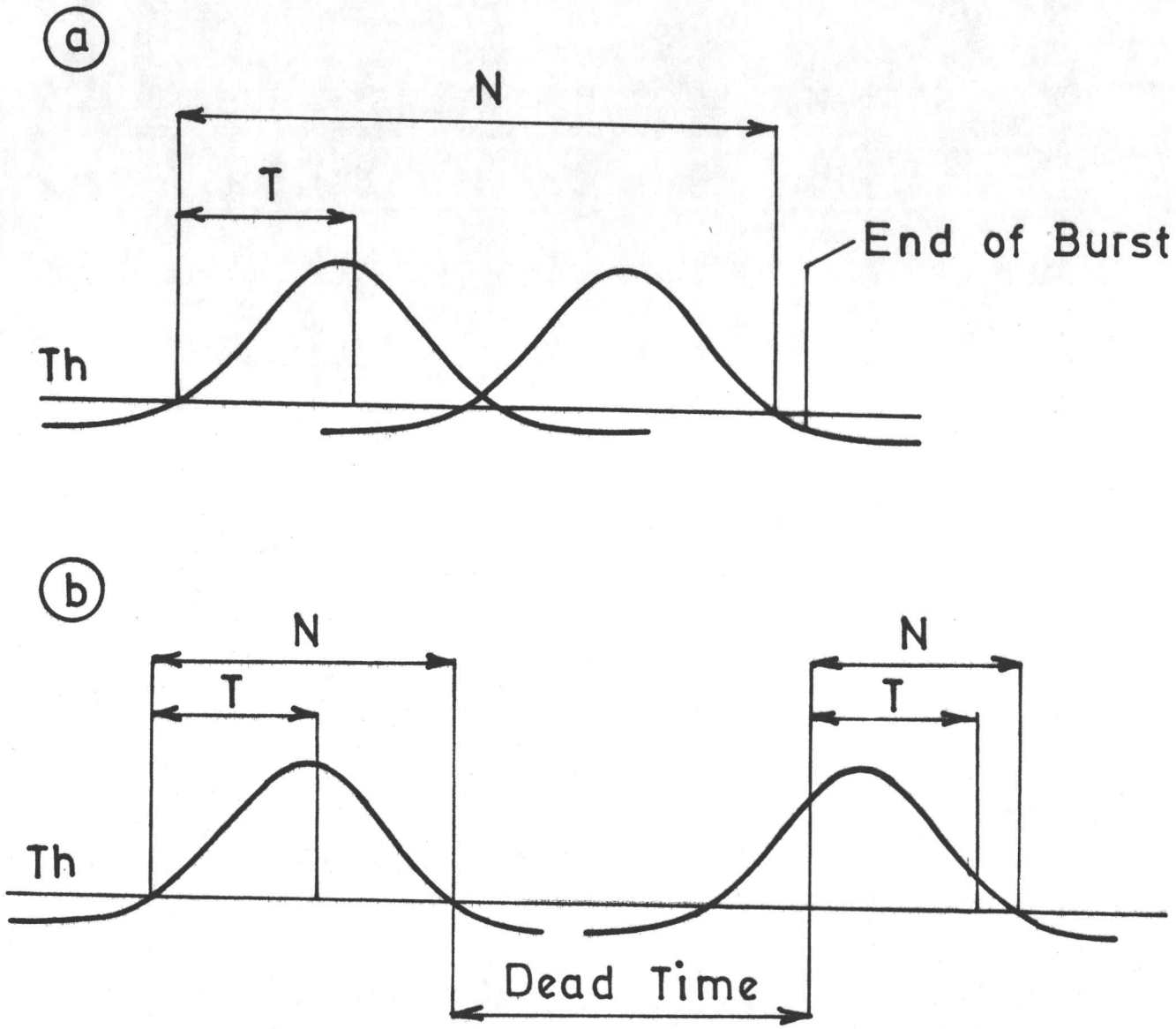

FIG. 19 - ERRORS ON CYCLE-COUNTING IN ACTUAL MEASUREMENTS

a) Error due to overlapping bursts : no EOB after the first burst
b) Error due to the dead time : count starts late on second burst